2026 • Vol. 1 • pp. x–xx • REPORT EARLY VIEW ARTICLE

Journal of Lost Species

Australyichthys gen. nov. (Teleostei, Syngnathidae), a lost mesophotic lineage from southern Australia, with description of *A. aegis* sp. nov. and reclassification of *Hippocampus minotaur* and *H. paradoxus*

Graham Short[1,2,3,4,5], Ralph Foster[6], Martin Gomon[7], Susan Bassham[8], Clayton M. Small[9], Kerryn Parkinson[1], Alexander DuToit[10], Christina Biggs[11], David Harasti[4,12], Healy Hamilton[4], and Amanda Hay[1]

[1]Ichthyology, Australian Museum Research Institute, 1 William Street, Sydney, NSW 2010, Australia
[2]Ichthyology, California Academy of Sciences, 55 Music Concourse Dr, San Francisco, CA 94118, United States
[3]Ichthyology, Burke Museum of Natural History and Culture, 4303 Memorial Way Northeast, Seattle, WA 98195, United States
[4]IUCN SSC Seahorse, Pipefish and Seadragon Specialist Group, Vancouver BC V6T 1Z4, Canada
[5]Visiting research fellow, University of Technology, Sydney, NSW 2007
[6]Ichthyology Section, South Australian Museum, North Terrace, Adelaide, South Australia, Adelaide 5000
[7]Ichthyology, Museum Victoria, GPO Box 666 Melbourne, Victoria 3001, Australia
[8]Institute of Ecology and Evolution, University of Oregon, Eugene, OR 97403, United States
[9]Department of Biological Sciences, Idaho State University, Pocatello, ID 83209, United States
[10]Department of Biology, University of Massachusetts, Amherst, MA 01003, United States
[11]BLUeDNA Institute, Monterey, CA 93940, United States
[12]Fisheries Research, Port Stephens Fisheries Institute, Taylors Beach, NSW, 2316, Australia

Abstract: *Australyichthys* gen. nov. is described as a new genus of Syngnathidae (seahorses, pipefishes, seadragons, pipehorses, and pygmy pipehorses) endemic to temperate mesophotic habitats of southern Australia and erected to include *A. minotaur* comb. nov. and *A. paradoxus* comb. nov., together with *A. aegis* sp. nov. The genus occurs at depths of 50–124 m within a mesophotic zone characterized by reduced light penetration and structurally complex benthic habitats. The included taxa possess hippocampiform features including a ventrally angled head, a fully enclosed brood pouch, and a prehensile tail, but are distinguished by a consistent osteological combination. Micro-computed tomography reveals an elevated, anteriorly inclined supraoccipital, a reduced anterior nuchal plate not forming a coronet, and unfused inferior trunk plates lacking a continuous ventral ridge. The external morphology is comparatively unsegmented,

Corresponding author: Graham Short, gshort@calacademy.org
Received: 28 February 2026 • Accepted: 8 July 2026 • Published: xxxxx 2026
Handling editor: Topiltzin Contreras-MacBeath

ISSN: 3070-6831
https://doi.org/10.66264/y1ffbcwb

with subtle dermal lobulation contributing to a fleshy habitus. A derived ventral trunk complex is present, composed of anterior and posterior ventral elements flanking a median anal pterygiophore, homologous to the anal-fin pterygiophore complex of *Hippocampus* but reorganized into a novel ventral support architecture not observed elsewhere in Syngnathidae. Phylogenomic analyses of ultraconserved elements recover *Australyichthys* within Haliichthyini, the sister clade to Hippocampini, indicating that the hippocampiform body plan arose independently of *Hippocampus* and reflects convergence rather than shared ancestry. The genus is represented by eight specimens collected incidentally over nearly eighty years, with no collections within the last two decades and no verified *in situ* observations, and therefore meets the criteria of a lost taxon. Its rarity, restricted depth range, and predominant occurrence in mesophotic habitats underscore the need for targeted surveys and formal conservation assessment.

Keywords: convergent evolution, Great Southern Reef, lost species concept, phylogenomics, southern Australia, systematics, taxonomy, temperate mesophotic ecosystems

Conservation statement: Our ability to assess the conservation status of *Australyichthys* is limited: the genus is known from only a few historical museum specimens and has never been observed in the wild, the most recent record being a 2006 trawl-bycatch specimen. We interpret this absence of recent records conservatively, as reflecting limited sampling of temperate mesophotic habitats rather than population decline or extirpation. Under the lost species framework, all three species qualify as lost, unrecorded for ten or more years. We have not undertaken a formal International Union for Conservation of Nature (IUCN) Red List assessment; available data are insufficient to support one, and the genus is best regarded as Data Deficient pending targeted, non-extractive surveys of southern Australian mesophotic habitats.

A second-language abstract and conservation statement are not provided. The distribution of *Australyichthys* gen. nov. spans the Sea Country of many First Nations across southern Australia, which cannot be fairly represented by any single language.

INTRODUCTION

Natural history

Australia is a global center of syngnathid (pipefishes, seahorses, seadragons, pipehorses, and pygmy pipehorses) diversity and endemism, harboring nearly half of all recognized genera and supporting 45 endemic species distributed across 16 endemic genera (Dawson 1985; Hamilton et al. 2017). Phylogenetic studies indicate that endemic taxa occur in all major clades, except the Atlantic (Hamilton et al. 2017; Stiller et al. 2022). Southern Australia alone accounts for 36 endemic species and 15 endemic genera, forming the core of a monophyletic radiation of temperate pipefishes that exemplifies ecological specialization and morphological diversification within Syngnathidae (Dawson 1985; Hamilton et al. 2017; Stiller et al. 2022). Much of this diversity occurs in shallow ecosystems dominated by fucoid algae and extensive seagrass meadows, which constitute the best-documented syngnathid habitats in the region (Dawson 1985; Martin-Smith 2003; Browne et al. 2008; Moore et al. 2024). In contrast, southern Australia's temperate mesophotic ecosystems, spanning approximately 30–150 m depth, remain poorly represented in collections. Mesophotic ecosystems exhibit distinct ichthyofaunal assemblages, elevated endemism, and ecological structure that differ markedly from shallow reef systems (Bongaerts and Smith 2019; Bridge et al. 2013; Loiseau et al. 2023; Turner et al. 2019), and remain among the least studied marine habitats globally.

Australyichthys is the first syngnathid genus documented predominantly from the temperate mesophotic ecosystems of southern Australia (Dawson, 1985), with all records to date between 50 and 124 m depth. The genus is diagnosed by morphological characters consistent across all known specimens. Dorsal dermal lobes are recurrent external features within the genus; their functional role remains unknown, although they may facilitate crypsis within structurally complex benthic habitats.

All verified records of *Australyichthys* occur at mesophotic depths based on available collection data, in contrast to the predominantly shallow-water syngnathid fauna of southern Australia's coastal shelf. Temperate mesophotic ecosystems (TMEs), defined here as approximately 30–150 m depth, exhibit faunal assemblages and habitat structure distinct from shallow reef systems (Bastiaansen et al. 2024; Bell et al. 2024; Beran 2024; Currey-Randall et al. 2021; Gragnolati et al. 2024; Turner et al. 2019; Williams et al. 2019; Wong et al. 2023). Despite this ecological significance, TMEs remain among the least studied components of Australia's marine biota. Whereas shallow syngnathid habitats are dominated by macroalgae and seagrass (Baker 2006; Browne et al. 2008; Dawson 1985; Last et al. 2011; Moore et al. 2024; Peter et al. 2011), the mesophotic zone along southern Australia's shelf comprises structurally complex biogenic habitats, including sponge gardens, bryozoan colonies, and coral-like assemblages. These habitat-forming taxa produce patchy, three-dimensional structures across calcareous and sedimentary substrates, a habitat configuration compatible with the occurrence of cryptobenthic taxa. All specimens of *Australyichthys* have been collected from depths and regions where such benthic assemblages are documented (Adams et al. 2023; Ahmadia et al. 2012; Bastiaansen et al. 2024; Bell et al. 2024; Brandl et al. 2018; Harris et al. 2021; Navarro et al. 2023). Trophic evidence from this study, though limited to a single specimen, provides the first direct evidence of diet; computed tomography (CT) scans of *A. paradoxus* revealed unidentifiable crustacean remnants within the digestive tract, indicating ingestion of small invertebrate prey.

Systematics

Taxonomic background and history

Two enigmatic syngnathids from the mesophotic depths of southern Australia have resisted taxonomic resolution since their original descriptions. *Hippocampus minotaur* Gomon, 1997 from New South Wales and *H. paradoxus* Foster & Gomon, 2010 from Western Australia exhibit external characters diagnostic of *Hippocampus*, including a ventrally angled head, prehensile tail, and enclosed brood pouch, yet both species possess morphological features inconsistent with that genus (Foster and Gomon 2010; Gomon 1997) (Fig. 1). These anomalies suggest that the resemblance to *Hippocampus* reflects external similarity rather than shared ancestry, warranting osteological reassessment. Resolution of their taxonomic placement has required comparative osteological and phylogenomic data that were previously unavailable.

The Syngnathidae comprises more than 300 species in 57 genera, including seahorses, pipefishes, pipehorses, seadragons, and pygmy pipehorses (Dawson 1985; Hamilton et al. 2017; Stiller et al. 2022). Phylogenetic analyses based on multilocus and ultraconserved element datasets have resolved several principal radiations, providing a framework of major clades for evaluating morphological evolution and biogeographic structure across the family. One such division separates the sister tribes Hippocampini (which includes *Hippocampus*) and Haliichthyini, an Indo-Pacific assemblage of pipefishes and pygmy pipehorses (Hamilton et al. 2017; Stiller et al. 2022). Members of Haliichthyini exhibit extensive variation in overall morphology, ranging from ground-dwelling pipefishes to pygmy pipehorses with prehensile tails (Hamilton et al. 2017; Short and Trnski 2021; Stiller et al. 2022).

Consistent with the poor representation of temperate mesophotic taxa in museum collections, *H. minotaur* and *H. paradoxus* are known collectively from only six specimens collected between 64 and 124 m depth. Gomon (1997) described *H. minotaur* as possessing an enlarged fleshy head, complete absence of spination, atypical development of mid-dorsal dermal lobes, and undeveloped ventral trunk ridges. Foster and Gomon (2010) provided additional osteological details for *H. paradoxus* from CT scans, including a reduced anterior

nuchal plate, modified inferior trunk plates, a complex of ventral ossifications near the anal region, and a posteriorly expanded abdomen visible through the integument. The taxonomic placement of these species remained unresolved, limited by few specimens and the absence of comparative osteological data, which together constrained morphological comparison and the phylogenomic analyses needed to resolve their placement within Syngnathidae. Although *H. paradoxus* was examined using CT (Foster and Gomon 2010), equivalent imaging data were unavailable for *H. minotaur*, precluding detailed skeletal comparison. The absence of phylogenomic data and comparative material from additional taxa prevented assessment of whether shared morphological features reflected divergence within *Hippocampus* or affiliation with an independent lineage.

Resolution of this lineage was enabled by the discovery of a specimen from the entrance to Spencer Gulf, South Australia, here described as a new species. This material bridges the geographic gap between the New South Wales and Western Australian taxa, spanning more than 2,500 km of the southern Australian coastline, and permits explicit evaluation of whether the anomalous characters documented in *H. minotaur* and *H. paradoxus* are shared across the lineage. Osteological comparison demonstrates that these features are conserved across all examined specimens and together define a morphologically cohesive group.

High-resolution CT of all three species, together with genome-scale phylogenomic data from the Spencer Gulf specimen, permit reassessment of this lineage within Syngnathidae, and provides an integrated framework for interpreting its morphology in a broader phylogenetic context. Osteological features distinguishing this group from *Hippocampus* include modifications of the supraoccipital, anterior nuchal plate, and inferior trunk plates, and a derived ventral trunk complex without counterpart in *Hippocampus*. Among these features, modifications of the ventral trunk are the most diagnostic, as they involve discrete skeletal reorganization, rather than external body shape. In particular, the ventral trunk incorporates a highly modified anal-fin–associated support system integrated with novel ventral ossifications, which together constitute the primary evidence for generic distinction. The combination of external seahorse-like characters with this unique ventral trunk architecture does not correspond to any recognized syngnathid body plan, including those of seahorses, pipefishes, pipehorses, seadragons, or pygmy pipehorses. This lineage accordingly represents a novel morphological configuration within Syngnathidae.

Our UCE-based phylogenomic analyses, described in detail below, place this lineage within Haliichthyini, an Indo-Pacific assemblage of pipefishes and pygmy pipehorses previously resolved as the sister clade to Hippocampini (Hamilton et al. 2017; Stiller et al. 2022). This robustly supported pattern demonstrates that seahorse-like external morphology has evolved independently within both tribes. We examine the anatomical basis of this convergence, and its possible functional correlates, through comparative analysis of ventral architecture across Haliichthyini and Hippocampini.

We here formally recognize this lineage as *Australyichthys* gen. nov. and describe *A. aegis* sp. nov. from Spencer Gulf. Morphological, osteological, and phylogenomic evidence supports the validity of the genus and reveals previously unrecognized diagnostic characters, including synapomorphies of the ventral trunk region that permit comparative assessment of skeletal organization between Haliichthyini and Hippocampini. The restriction of *Australyichthys* to temperate mesophotic ecosystems, together with its extreme rarity in collections, constrains inference about its distribution, population status, and ecological associations, and bears directly on the conservation assessment presented here.

The taxonomic history of *A. minotaur* and *A. paradoxus* has been shaped by interpretations of the traditional character suite used to delimit *Hippocampus*, most notably the ventral-

ly angled head, prehensile tail, and fully enclosed brood pouch. Reliance on these external features led Gomon (1997) to originally assign *H. minotaur* to *Hippocampus*, proposing affinity with the pygmy seahorse *H. bargibanti* based on shared reductions in ventral ossification, dorsal lobe development, and apparent truncation of the ventral trunk structure. However, Foster and Gomon (2010) interpreted the brood pouch of *H. minotaur* as conforming to the Type V configuration *sensu* Wilson et al. (2001) based on external morphology, aligning it with non-pygmy seahorses rather than the pouch morphologies typical of pygmy taxa. Their assessment predated detailed comparative evaluation of ventral trunk osteology; the present study shows that this resemblance reflects external similarity to the Type V pouch of *Hippocampus* rather than a shared reproductive synapomorphy, removing the principal character previously used to argue affinity with pygmy seahorses.

Lourie and Kuiter (2008) noted the unusual morphology of *H. minotaur*, including enlarged dorsal dermal lobes, absence of cranial and trunk spination, an apparently discontinuous cleithral profile, and atypical cranial proportions, and highlighted that these characters did not conform to diagnostic expectations for *Hippocampus*. Foster and Gomon (2010) further emphasized the incongruity between seahorse-like external morphology and internal skeletal structure in both *H. minotaur* and *H. paradoxus*. Although CT was employed in the description of *H. paradoxus*, the observed osteological characters were examined under the assumption that the species belonged to *Hippocampus*. As a result, these characters were not analyzed in the comparative detail presented here and were instead interpreted as species-level modifications within *Hippocampus*.

The current study re-evaluates these structures within a comprehensive comparative context, revealing that the osteological organization of *Australyichthys* is incompatible with *Hippocampus*. The anterior nuchal plate is vestigial and free-floating rather than integrated into the continuous supraoccipital–nuchal complex typical of non-pygmy seahorses. In *A. paradoxus*, the apparent prominence of this element reflects positional and integumentary effects rather than osteological development. The ventral trunk region of *Australyichthys* possesses a derived, three-part anal-region support complex: anterior and posterior ventral elements (AVE, PVE) flanking a centrally positioned median anal pterygiophore (MAP) (Figs. 2, 3, 4, 5). In *Hippocampus*, the anal region is supported exclusively by the anal fin pterygiophore complex expressed as multiple radials, which retain a fin-support role and are not reorganized into discrete anterior or posterior ventral elements flanking a median element.

Materials and methods

Material examined. All available type and non-type specimens of *A. minotaur*, *A. paradoxus*, and *A. aegis* were examined from the ichthyological collections of Museums Victoria (NMV), the Australian Museum (AMS), the South Australian Museum (SAMA), the Commonwealth Scientific and Industrial Research Organisation (CSIRO), and the California Academy of Sciences (CAS). These specimens formed the basis for all genetic, morphological, meristic, micro-computed tomography (CT), and comparative assessments conducted in this study.

Material examined for *A. minotaur* includes the holotype NMV A192 (male, 48.7 mm SL), paratypes AMS IA.3509 (female, 42.2 mm SL) and AMS IA.3560 (female, 52.6 mm SL), and non-type specimens CSIRO H4464-01 (male, 53.9 mm SL) and CAS 13403 (male, 33.7 mm SL). *Australyichthys paradoxus* is represented by the holotype SAMA F10490 (female, 64.6 mm SL). *Australyichthys aegis* is represented by the holotype SAMA F14993 (male, 56.0 mm SL).

The examined material is predominantly housed in Australian ichthyological collections (CSIRO, AMS, SAMA, NMV), with the exception of a single *A. minotaur* specimen deposited at CAS.

Institutional abbreviations follow Sabaj (2020). Taxonomic nomenclature follows Yearsley et al. (2006), Hoese et al. (2006), Gomon et al. (2008), and Neira et al. (1998). The comparative material examined from other syngnathid taxa, which provided the basis for the osteological comparisons presented below, is listed in the following entries.

Hippocampus erectus, UF 138664; Honduras, Caribbean Sea, Pink Shrimp grounds off Caratasca; 15.933°N, 83.683°W, depth 0 m; 12 April 1967; R/V Shady Lady (station 6703.15.933).

Acentronura gracilissima, CAS 81986; Japan, Pacific Ocean, NW and Central Pacific, Sagami-nada (Sagami Sea), Misaki, Honshu Island, 35.16°N, 139.49°E (2 dp; ~14 km uncertainty on record); marine; 1900; D. S. Jordan and J. O. Snyder.

Halicampus grayi (identified as *Halicampus grayi*; catalogued as *Hippichthys penicillus*), LSUMZ 18017 Kuwait, Kuwait Bay (Persian Gulf); 5 June 2014; P. Chakrabarty and J. Bishop.

Haliichthys taeniophorus, SIO 09-362, Australia, Western Australia, Indian Ocean, near Shark Bay, 25.500°S, 113.500°E, captive bred (sampling protocol), Dallas World Aquarium.

External morphology and meristics. External measurements were taken following Dawson (1985) and are expressed as percentages of standard length (SL) or head length (HL). Meristic counts follow Lourie and Randall (2003), with modifications outlined by Foster and Gomon (2010) for interpretation of trunk ring boundaries and fin-support elements. Measurements were obtained using digital calipers to the nearest 0.1 mm.

Specimens were examined under a Leica MZ16 stereomicroscope. Digital images were captured using a Canon EOS 5D camera fitted with a 50 mm macro lens. Terminology for external morphology follows Dawson (1985), with additional clarification from Foster and Gomon (2010) and Short and Trnski (2021). Characters were assessed across all diagnostically relevant body regions, including the head, trunk, tail, dermal ornamentation, and fin-support structures.

Osteology and micro-computed tomography. High-resolution CT was conducted at the Karel F. Liem BioImaging Center, Friday Harbor Laboratories, University of Washington. Scans were performed using a Bruker SkyScan 1173 system equipped with a 1 mm aluminum filter, operated at 65 kV and 123 μA. Image stacks were acquired at 2048 × 2048 pixel resolution with isotropic voxel sizes ranging from 8 to 12 μm, depending on specimen size.

Specimens were scanned in ethanol and stabilized within 15 ml plastic tubes using ethanol-moistened cheesecloth to minimize movement. Reconstructions were generated using NRecon software. Volumetric datasets were visualized and examined using 3D Slicer v.5.10.10 with the SlicerMorph extension (Kikinis et al. 2013; Rolfe et al. 2021).

Skeletal structures were examined in dorsal, lateral, and ventral views and in three dimensions to document their configuration and associations. Ring counts, fin-ray counts, and spatial relationships among trunk, tail, and fin-support elements were derived directly from CT reconstructions.

Comparative CT data from *Hippocampus erectus* were examined to document the arrangement and position of trunk elements, fin-support structures, and ventral skeletal components for comparison with the corresponding structures in *Australyichthys*.

Phylogenomic data and analyses. Genomic DNA was extracted from tail tissue of *Australyichthys aegis* sp. nov. (holotype SAMA F14993; tissue bank registration number ABTC137691), fixed in ethanol, using the DNeasy Blood and Tissue Kit (Qiagen, Inc.) following the manufacturer's protocol, with extended lysis to maximize total yield. Extractions were conducted at the Australian Centre for Wildlife Genomics (ACWG), Australian Museum. DNA integrity was assessed by agarose gel electrophoresis and an Agilent TapeStation 4200, and DNA

concentration was quantified using a Qubit 3.0 fluorometer.

An Illumina-compatible shotgun genomic library was constructed by the University of Oregon Genomics and Cell Characterization Core Facility. Library quality and fragment-size distribution were evaluated using an Agilent 2100 Bioanalyzer. Sequencing was performed on an Illumina NovaSeq 6000 platform using paired-end 150 base-pair reads, yielding 101,723,675 whole-genome shotgun reads.

The whole-genome shotgun reads generated for *A. aegis* were used directly as input to PhyloAln v1.0.0 (Huang et al. 2024), which aligns short-read sequencing data onto existing reference alignments, allowing a newly sequenced taxon to be incorporated into an established phylogenomic dataset without *de novo* assembly. Newly generated genomic data for *A. aegis* will be deposited in GenBank upon acceptance.

Existing UCE alignments for syngnathid fishes published by Stiller et al. (2022) were obtained from the EMBL-EBI BioProject PRJNA734786. From these datasets, UCE sequences from twenty-two species spanning 15 genera were selected to represent phylogenetic diversity across the Stiller et al. (2022) species trees, and included seven species of *Hippocampus*. Of the published UCE alignments, 271 loci contained sequences from all selected comparator taxa (Table 1). These loci were combined with newly generated data for *A. aegis* to produce a23-species alignment.

Table 1. List of species and sample accession numbers for ultraconserved element (UCE) genomic sequences analyzed in this study. All sequences were obtained from Stiller et al. (2022) (EMBL-EBI BioProject PRJNA734786).

Species	Sample accession
Acentronura tentaculata	SAMN19535364
Amphelikturus dendriticus	SAMN19535366
Corythoichthys intestinalis	SAMN06563050
Doryrhamphus excisus	SAMN19535409
Filicampus tigris	SAMN19535434
Halicampus grayi	SAMN19535438
Halicampus macrorhynchus	SAMN19535440
Haliichthys taeniophorus	SAMN19535445
Hippocampus bargibanti	SAMN19535461
Hippocampus denise	SAMN19535472
Hippocampus pontohi	SAMN19535494
Hippocampus jugumus	SAMN19535483
Hippocampus abdominalis	SAMN19535457
Hippocampus white	SAMN19535510
Hippocampus zosterae	SAMN12912696
Micrognathus crinitus	SAMN19535530
Idiotropiscis lumnitzeri	SAMN19535518
Leptonotus elevatus	SAMN19535523
Lissocampus filum	SAMN19535526
Phycodurus eques	SAMN14574976
Syngnathus scovelli	SAMN19535597
Trachyrhamphusbicoarctatus	SAMN19535603

Phylogenetic inference was conducted using both concatenated and coalescent-based approaches. Maximum Likelihood analyses were performed in IQ-TREE2 v2.4.0 (Minh et al. 2020) under default settings, with ModelFinder (Kalyaanamoorthy et al. 2017) selecting a single best-fitting nucleotide-substitution model for the concatenated matrix, with nodal support assessed using 1000 ultrafast bootstrap replicates (Hoang et al. 2018). For the coalescent-based analysis, a separate gene tree was inferred for each of the 271 loci in IQ-TREE2 under the same settings, and these gene trees were summarized into a species tree using weighted ASTRAL (wASTRAL v1.20.3.7; Zhang and Mirarab 2022), which accommodates gene-tree uncertainty through branch-support and branch-length weighting, with local posterior probabilities (Sayyari and Mirarab 2016) calculated for each node. *Doryrhamphus excisus* was specified as the single outgroup for all analyses. The concatenated ML tree and the wASTRAL species tree were drawn and labelled in FigTree v1.4.4 (Rambaut 2010).

The resulting phylogenetic hypotheses were used to evaluate the placement of *Australyichthys* within Syngnathidae and to assess its relationship to *Hippocampus* and other Indo-Pacific pipefish lineages.

Taxonomic account

***Australyichthys* Short, Foster & Gomon, gen. nov.** Diagnosis. A genus of Syngnathidae distinguished from all other syngnathid genera by a derived ventral trunk support complex—comprising anterior ventral elements (AVE), paired posterior ventral elements (PVE), and a single median anal pterygiophore (MAP) positioned between them—that provides ventral support in place of the midline plate contact present in other syngnathids. This reorganization of ventral trunk support, rather than any particular configuration of its component elements, is the genus-level synapomorphy; the detailed configuration of the complex varies among species (the AVE is a single median series in *A. minotaur* but paired in *A. paradoxus* and *A. aegis*; the PVE is unfused in *A. minotaur* and *A. paradoxus* but proximally fused in *A. aegis*) and is treated as species-level variation in the accounts below. The genus is further distinguished by ventral plates absent and inferior trunk plates unfused along the ventral midline, so that a continuous ventral trunk ridge is lacking; anterior nuchal plate reduced and not integrated with the supraoccipital, failing to form a coronet; supraoccipital highly elevated; superior and lateral trunk plates fused; and spination absent. Externally, the genus resembles *Hippocampus* in the ventrally angled head (axis approximately 90° to the trunk), prehensile tail, absent caudal fin, and fully enclosed male brood pouch, but differs from that genus in the reduced anterior nuchal plate (vs. a coronet formed by integration of the supraoccipital and anterior nuchal plate), the unfused inferior plates and absent ventral plates (vs. inferior and ventral plates meeting at the ventral midline to form a rigid enclosure), and the consolidation of the anal-fin pterygiophore complex into the median MAP integrated into ventral trunk support (vs. three discrete radials retaining a fin-support role). The head is large and fleshy, with a short snout; the cleithrum is robust; the first vertebra has a bifurcated anterior margin; the body is externally soft and unsegmented, with ring boundaries obscured; the mid-dorsal dermal lobes are aligned along the dorsal midline and unsupported by bony processes, ranging from well developed to reduced or absent among species. Dorsal fin variably present: present in *A. minotaur* (seven rays on five pterygiophores, restricted to the first tail ring) (Fig. 6), absent together with all associated pterygiophores in *A. paradoxus* and *A. aegis*. Pectoral-fin rays 10–11; anal-fin rays 4 or fewer, vestigial or absent in adults; trunk rings 8; tail rings 38–42. Embryos in males positioned beneath the PVE–MAP complex; hydrated oocytes in females within the abdominal cavity between the AVE and PVE. Standard length 33.7–64.6 mm.

The type species is *Australyichthys minotaur* (Gomon, 1997), by original designation.

The genus name is a neologism derived from the Latin *australis* (southern), referencing the geographic restriction of the genus to southern Australia, and the Greek *ichthys* (fish), reflecting its taxonomic placement within the family Syngnathidae; gender masculine.

Common English name. Sea Muppet. The common name "sea Muppet" reflects the appearance of the genus, with its large, prominently domed head and fleshy lobes evoking features reminiscent of the animated characters from The Muppet Show.

Remarks. The original assignment of *Hippocampus minotaur* and *H. paradoxus* to *Hippocampus* was based primarily on external morphology; osteological interpretation was constrained by the limitations of radiography and by difficulty resolving fine skeletal structure through dense integument (Foster and Gomon 2010; Gomon 1997). Externally, members of *Australyichthys* possess features that contributed to this historical assignment, including an angled neck relative to the body, a fully enclosed male brood pouch, and a prehensile tail, characters traditionally associated with *Hippocampus*. A series of dermal lobes arranged strictly along the dorsal midline, extending from the first trunk ring

onto the tail (Figs. 1, 3, 7, 8, 9), reinforced the seahorse-like appearance. These lobes are unsupported by bony processes and therefore differ from spine-supported lobes of seadragons (*Phyllopteryx*, *Phycodurus*) and from the dorsolateral filamentous appendages of *Haliichthys taeniophorus*. The series of medially aligned lobes described for *A. paradoxus* and *A. aegis* includes trunk and tail lobes that superficially resemble fins but lack fin rays and fin supports, consistent with interpretation as integumentary outgrowths, rather than fin derivatives (Foster and Gomon 2010) (Fig. 10). Because molecular data could be obtained only from *A. aegis*, the transfer of *A. minotaur* and *A. paradoxus* to *Australyichthys* rests on the shared osteological synapomorphies of the genus rather than on sequence data from those two species (Figs. 11, 12).

CT reveals osteological characters that distinguish *Australyichthys* from *Hippocampus*, allowing direct evaluation of whether external similarity is underpinned by shared skeletal structure. In *Hippocampus*, the coronet is formed by structural integration of the supraoccipital and anterior nuchal plate (Figs. 13–15). In *H. paradoxus*, Foster and Gomon (2010) reported that the coronet was only evident in radiographs, as diffuse ossification lying between the supraoccipital and the first nuchal plate, and not in contact with the supraoccipital. CT in the present study resolves this morphology as a reduced anterior nuchal plate that lacks the structural integration required to form a discrete coronet (Figs. 2, 8, 10). In *Australyichthys*, reduction of the anterior nuchal plate precludes coronet formation. CT also reveals that the skeletal structure of the ventral trunk lacks a continuous ventral ridge formed by fused inferior plates (Figs. 2, 4, 8, 10). This contrasts with the ventral trunk in *Hippocampus*, in which inferior plates meet along the ventral midline to form a continuous ridge and contribute to complete ossification support of the trunk (Figs. 13–15). In *A. paradoxus*, Foster and Gomon (2010) described thoracic rings that almost encircle the trunk but remain unfused ventrally, with the ventral trunk ridge absent, and noted scaffold-like ossified elements associated with the last trunk ring; these observations are consistent with CT-based interpretation of reduced ventral trunk ossification, in which discrete ventral ossifications (AVE, PVE, MAP) provide structural support, rather than midline fusion of ventral plates (Figs. 2, 4, 5, 8, 10). The superior trunk ridges also differ: in *A. paradoxus* and *A. aegis*, the superior trunk ridges are elevated, whereas in *Hippocampus* superior trunk ridges lack elevations and instead bear spines (Figs. 13–15).

Among all examined skeletal regions, the ventral trunk support complex provides the clearest osteological evidence for generic distinction of this lineage. The principal synapomorphy of *Australyichthys* is a derived ventral trunk support system comprising anterior ventral elements (AVE), posterior ventral elements (PVE), and a centrally positioned median anal pterygiophore (MAP). The AVE are expressed as a single median multisegmented series in *A. minotaur* (Figs. 2, 4, 5) and as paired multisegmented series in *A. paradoxus* and *A. aegis* (Figs. 8, 10). The AVE arise from the inferior plates, whereas the PVE originate from plate elements of the final trunk ring and are interpreted as modified inferior plate derivatives. Together with the MAP, the AVE and PVE reorganize ventral support in the absence of a midline ventral ridge. The presence of this reorganized complex is shared by all three species and diagnoses the genus, whereas the differing configurations of its elements (the AVE median or paired; the PVE unfused or proximally fused) distinguish the species.

The median anal pterygiophore (MAP) is a cylindrical ossification with a bulbous terminus, positioned centrally between the AVE and PVE (Figs. 2, 4, 5, 8, 10). Homology of the MAP is inferred on the basis of positional correspondence within the ventral trunk series, consistent spatial relationships to the AVE and PVE, and shared internal structural features revealed by CT. Its homology is interpreted through comparison with *Hippocampus*, in which the anal fin support comprises three

proximal pterygiophores, each constructed from serial radial segments—proximal and distal radials (Dudley et al. 2022; Schneider et al. 2023). In *Hippocampus abdominalis*, Dudley et al. (2022) documented the distal ends of the proximal pterygiophore segments as a continuous lobed cartilage based on histological staining, describing them as "fused middle radials"; the same fused morphology is corroborated here by CT observations of *Hippocampus erectus* (Figs. 13–15). In *Hippocampus*, the proximal radials terminate ventrally in fused ends that articulate with the corresponding inferior plates of the posterior-most trunk ring; the distal radials serve as fin ray articulation sites. In the CT reconstruction of the adult *H. erectus*, the anal fin pterygiophore complex appears as a partially fused or incompletely subdivided structure in which the termini of the proximal radials are laminated together in a stacked arrangement with two horizontal grooves that mark the boundaries between the three radials; proximal to this fused end, the radials remain separated from each other as smooth rods (Fig. 14C).

In *Australyichthys*, only a single median anal pterygiophore is apparent; however, CT data reveal this element has a complex, horizontally grooved topography suggesting consolidation of more than one pterygiophore element (Figs. 2, 8, 10). As in *Hippocampus*, *A. minotaur* has four anal-fin rays, though these are variably present. We therefore hypothesize that the singular anal pterygiophore structure (MAP) in *Australyichthys* could have resulted from incomplete separation, or from secondary fusion, of more than one proximal radial cartilage element during development of the anal pterygiophores, laminating them together along their length (Figs. 2D, E). A horizontal groove in the bulbous end of the structure might mark the boundary between two radial elements. In the absence of developmental or ontogenetic series, we offer this as the most parsimonious interpretation of the CT evidence rather than a confirmed homology. Accordingly, the MAP of *Australyichthys* is interpreted as corresponding positionally and structurally to the seahorse anal fin pterygiophore complex, while being expressed as a single midline element integrated into the ventral trunk support system, rather than as three discrete pterygiophores associated with fin ray articulation as in *Hippocampus*. Its position relative to the brood pouch is compatible with a mechanical role in pouch deformation during parturition (cf. Dudley et al. 2022).

The ventral trunk support complex is integrated with reproductive anatomy. In males, a fully enclosed brood pouch is present along the ventral midline of the posterior trunk and extends onto the anteriormost caudal rings (Figs. 1, 3, 9). In females, a brood pouch is absent; hydrated oocytes are present within the abdominal cavity between the AVE and PVE (Figs. 3, 5, and 8). In *A. minotaur* males, brooded embryos are present beneath the combined PVE–MAP complex.

Sexual dimorphism is documented most clearly in *A. minotaur*, in which differences occur in the supraoccipital, AVE, and PVE. The supraoccipital is highly elevated in both sexes, but males exhibit a more steeply angled supraoccipital than females (Figs. 2, 4). In the AVE, males possess four ossified units, whereas females retain two elongate ossified units, all associated with the ventral plate of the third trunk ring (Figs. 2, 4, 5). In males, the PVE form paired elongate, rod-like ossifications attached to the lateral plates at trunk ring 8; in females, the PVE are broader and spatulate, with distal contact and fusion involving the MAP (Figs. 4, 5). In *A. paradoxus*, only the female holotype is available; the PVE are broad and unfused, flanking a free MAP (Fig. 8), a configuration consistent with the female morphology observed in *A. minotaur*. In *A. aegis*, only the male holotype is available; the PVE are proximally fused and diverge distally, enclosing the MAP between their terminal ends (Fig. 10), a configuration that differs from males of *A. minotaur* and may represent species-level variation or an alternative male morphology. Whether comparable sex-specif-

ic variation occurs in *A. paradoxus* and *A. aegis* remains unknown pending acquisition of additional specimens.

Dorsal fin expression varies within the genus. *Australyichthys minotaur* retains a dorsal fin with seven rays supported entirely by the first tail ring and by five dorsal fin pterygiophores (Fig. 6), whereas *A. paradoxus* and *A. aegis* lack the dorsal fin and associated pterygiophore elements. Complete absence of the dorsal fin in adults, as in *A. paradoxus* and *A. aegis*, is uncommon within Syngnathidae but is not unique. It also characterizes the "finless" pipefishes (*Penetopteryx* and *Apterygocampus*; Dawson and Allen 1978) and the pughead pipefishes (*Bulbonaricus*), in which adults lack the dorsal and pectoral fins. In these taxa the dorsal fin is present in larvae and lost during development (Dawson and Allen 1978), and the finless condition co-occurs with a cryptic, largely sedentary existence within coral, rubble, or other structurally complex microhabitats—an ecological parallel consistent with the loss inferred here for *Australyichthys*. Restriction of the dorsal fin base to the first tail ring contrasts with *Hippocampus*, in which the dorsal fin base commonly extends across both trunk and tail rings (Figs. 13–15). The loss of the dorsal fin in *A. paradoxus* and *A. aegis* may reflect reduced dependence on active locomotion in species closely associated with structurally complex mesophotic habitats. If these species are largely sedentary and rely on crypsis within bryozoan, sponge, or soft coral assemblages, the locomotory function of the dorsal fin may be under relaxed selection, facilitating its loss. This contrasts with *Hippocampus bargibanti*, which retains its dorsal fin despite an obligate association with gorgonian corals of the genus *Muricella*, suggesting that host specificity alone does not predict dorsal fin loss (Baine et al., 2008; Lourie and Randall, 2003; Smith et al., 2012). We present this scenario as a hypothesis: direct observations of habitat use and behavior are lacking, and the contrast with *Hippocampus bargibanti* is suggestive rather than conclusive. Retention of the dorsal fin in *A. minotaur* may indicate less specialized habitat use or greater reliance on fin-mediated movement.

Gomon (1997) proposed a close relationship between *Hippocampus minotaur* and *H. bargibanti* based on shared reductions in external segmentation and ventral trunk ridges, and noted that in *H. bargibanti* the ventral belly ossifications are reduced to disconnected star-like plates, whereas in *H. minotaur* dermal ossifications were described as absent ventrally, with a crescentic process in radiographs of females (Gomon 1997). The present study does not support a close relationship between *Australyichthys* and *H. bargibanti*. The ventral skeletal organization of *Australyichthys* comprises a derived AVE, PVE, and MAP complex, whereas the ventral trunk in *H. bargibanti* is characterized by reduced, discontinuous ventral ossifications rather than a discrete ventral support system (Gomon 1997). Additionally, standard lengths of examined *Australyichthys* specimens (33.7–64.6 mm SL) exceed those of pygmy seahorses, which rarely surpass 30 mm SL (Short et al. 2018, 2020).

Key to the species of Australyichthys
(external characters only)

1a. Dorsal fin present, with seven rays; mid-dorsal dermal lobes reduced, variably developed, or absent ..... *A. minotaur*

1b. Dorsal fin absent 2

2a. Mid-dorsal dermal lobes broad and square-shaped; superior trunk ridges elevated on trunk rings 1–3 ... *A. paradoxus*

2b. Mid-dorsal dermal lobes sharply triangular and laterally compressed, consisting of a single large trunk lobe followed by six progressively smaller tail lobes; superior trunk ridges elevated on all trunk rings ..... *A. aegis*

***Australyichthys minotaur* (Gomon, 1997)**
Short, Foster & Gomon, comb. nov.
(Figs. 1–6)

Common name: bullneck sea Muppet.

Hippocampus minotaur Gomon, 1997: 245–253, Figs. 1–3; Kuiter, 2001: 304–305 (part); Foster and Gomon, 2010: 64; Lourie et al., 2016: 33 (part).
Holotype. NMV A192, male, 48.7 mm SL; Australia, New South Wales, off Eden, 64–73 m depth, 30 December 1960, Danish seine trawl, collected by R.J. Slack-Smith.
Paratypes. AMS IA.3560, female, 52.6 mm SL, 13 km east of Eden, 91.5–109.8 m depth, 37.00°S, 150.00°E, 1927, collected by H. Howell; AMS IA.3509, female, 42.2 mm SL, coast of New South Wales, trawl.
Other material. CAS 13403, male, 33.7 mm SL; Australia, New South Wales, 8 miles east of Eden, 73 m depth, 37.066°S, 150.055°E, October 1941, Danish seine trawl, collected by J.A. Tubb. CSIRO H4464-01, male, 53.9 mm SL; Australia, New South Wales, east of Disaster Bay (south of Eden), 124 m depth, 37.317°S, 150.277°E, 10 December 1996, collected by D. Gledhill.

Diagnosis. Australyichthys minotaur is distinguished from its congeners *A. paradoxus* and *A. aegis* by the combination of a dorsal fin present (seven rays on five robust pterygiophores positioned entirely on the first tail ring), versus dorsal fin and associated pterygiophores absent in both congeners; the AVE is a single median multisegmented series, versus paired in both; superior trunk ridges are not elevated, versus elevated in both; and mid-dorsal dermal lobes are reduced or absent, versus well developed and distinctly shaped in the congeners. Generic characters—the ventrally angled head, prehensile tail, absent caudal fin, enclosed male brood pouch, soft unsegmented body, and AVE–PVE–MAP ventral support complex—are given in the genus diagnosis above. The head is large and fleshy, with a short snout.

Figure 1. *Australyichthys minotaur*, NMV A192, holotype, male, 48.7 mm SL, freshly preserved, off Eden, New South Wales, Australia. Lateral view showing large fleshy head, soft externally unsegmented trunk and tail, and absence of spination. Photo credit, Martin Gomon.

The supraoccipital is highly elevated and anteriorly angled, more steeply inclined in males than in females. The anterior nuchal plate is vestigial and positioned between the supraoccipital and the first vertebra, lacking articulation with adjacent elements. The cleithrum is robust and dorsally expanded, extending anterior to the level of the first vertebra. The first

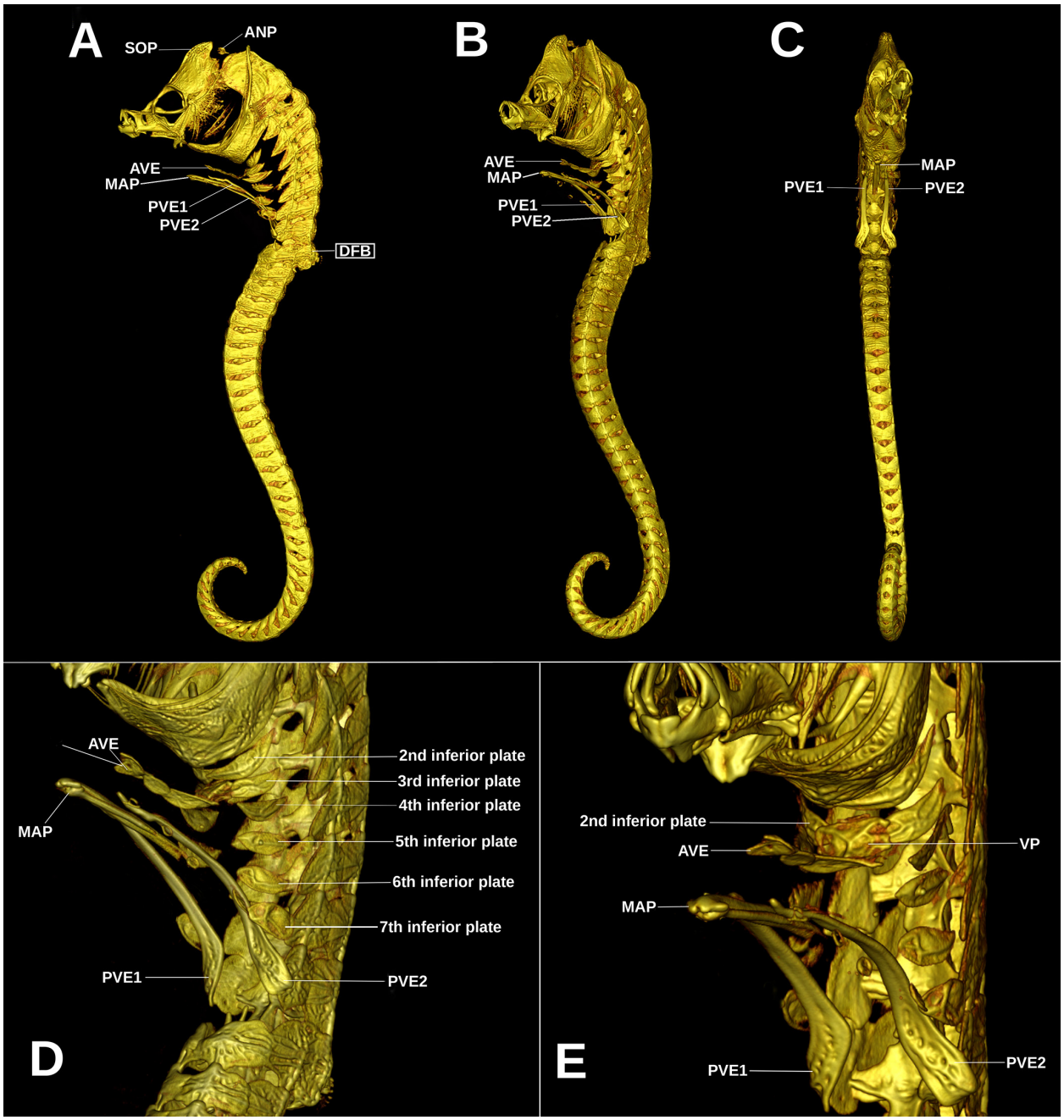

Figure 2. Micro-computed tomography (CT) scans of the skeleton of *Australyichthys minotaur*, NMV A192, holotype, male, 48.7 mm SL. (A) Lateral view. (B) Anterolateral view. (C) Anterior view. (D) Anterolateral trunk region showing the anterior ventral elements (AVE), median anal pterygiophore (MAP), posterior ventral elements (PVE), and inferior trunk plates (IP). (E) Anterolateral trunk region showing the second inferior trunk plates (IP), the median anal pterygiophore (MAP), and the ventral plate (VP). Abbreviations: AVE = anterior ventral elements; MAP = median anal pterygiophore; PVE = posterior ventral elements; IP = inferior plate; VP = ventral plate; ANP = anterior nuchal plate.

vertebra has a bifurcated anterior margin and a flattened dorsoposterior surface. The superior trunk ridges are not elevated, the superior and lateral plates are fused, and the inferior plates are unfused along the ventral midline. The inferior plates of the second trunk ring are elongate and interdigitate ventrally, whereas those of the remaining trunk rings are short and do not interdigitate. The ventral trunk region bears a derived support system comprising a single median anterior ventral element (AVE) and paired posterior ventral elements (PVE) that flank a centrally positioned median anal pterygiophore (MAP). The AVE is a multisegmented series of four ossified units in males and two elongate ossified units in females. The PVE is sexually dimorphic: in males it comprises elongate, curved ossifications with blunt distal termini, whereas in females it comprises broad, spatulate elements with scoop-like distal expansions fused at their margins, with the MAP fused between their terminal contacts. In males, the embryos are positioned beneath the PVE–MAP complex, whereas in females the hydrated oocytes lie within the abdominal cavity between the AVE and PVE. The pectoral-fin rays number 11, the anal-fin rays number 4 (vestigial or absent in adults), the trunk rings number 8, and the tail rings number 38–42.

Remarks. Australyichthys minotaur, the type species of the genus, establishes the anatomical framework for generic diagnosis. The species exhibits all generic characters: a large, fleshy head; soft, externally unsegmented trunk and tail lacking visible ring boundaries; 8 trunk rings; unfused inferior trunk plates; absence of spination; and minute mid-dorsal dermal lobes (Figs. 1–3), although these lobes are reduced or absent in some specimens. Extensive integumentary development obscures external skeletal segmentation, resulting in a highly modified external appearance relative to most syngnathids.

Gomon (1997:245–246) described this species as *Hippocampus minotaur* based on external morphology and radiographic examination, documenting a trunk and tail with extensive integumentary development, a markedly abbreviated snout, a coronet appearing as a low,

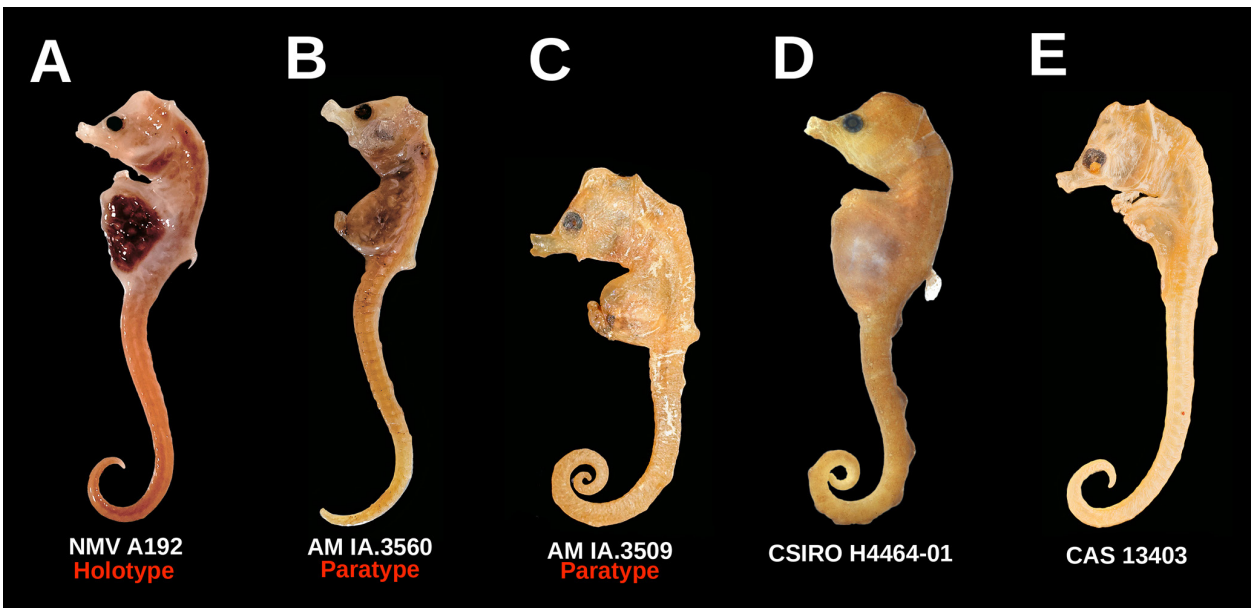

Figure 3. *Australyichthys minotaur*, preserved specimens from Eden, New South Wales, in lateral view. (A) NMV A192, holotype, male, 48.7 mm SL. (B) AMS IA.3560, paratype, female, 52.6 mm SL. (C) AMS IA.3509, paratype, female, 42.2 mm SL. (D) CSIRO H4464-01, non-type, male, 53.9 mm SL. (E) CAS 13403, non-type, male, 33.7 mm SL. Note variation in development of mid-dorsal dermal lobes across specimens. Photographs and CT images in this and subsequent figures by Graham Short unless otherwise noted.

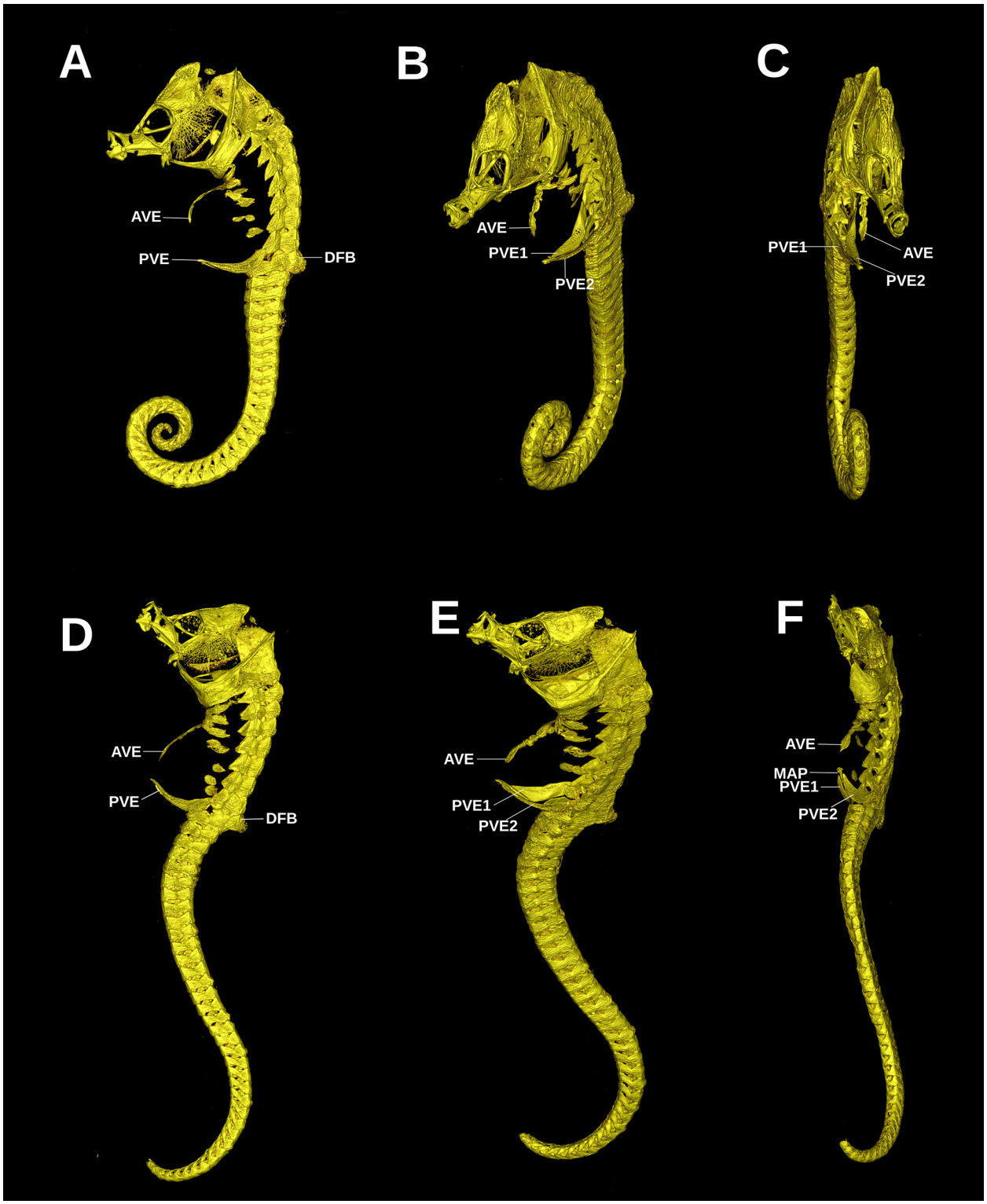

Figure 4. Micro-computed tomography (CT) scans of the skeletons of *Australyichthys minotaur*, female paratypes. (A–C) AMS IA.3560, 52.6 mm SL, in lateral, anterolateral, and anterior views. (D–F) AMS IA.3509, 42.2 mm SL, in lateral, anterolateral, and anterior views. Images show the anterior ventral elements (AVE), posterior ventral elements (PVE), median anal pterygiophore (MAP), and dorsal fin base (DFB). Note the broad, spatulate configuration of the PVE in females. Abbreviations: AVE = anterior ventral elements; PVE = posterior ventral elements; MAP = median anal pterygiophore; DFB = dorsal fin base.

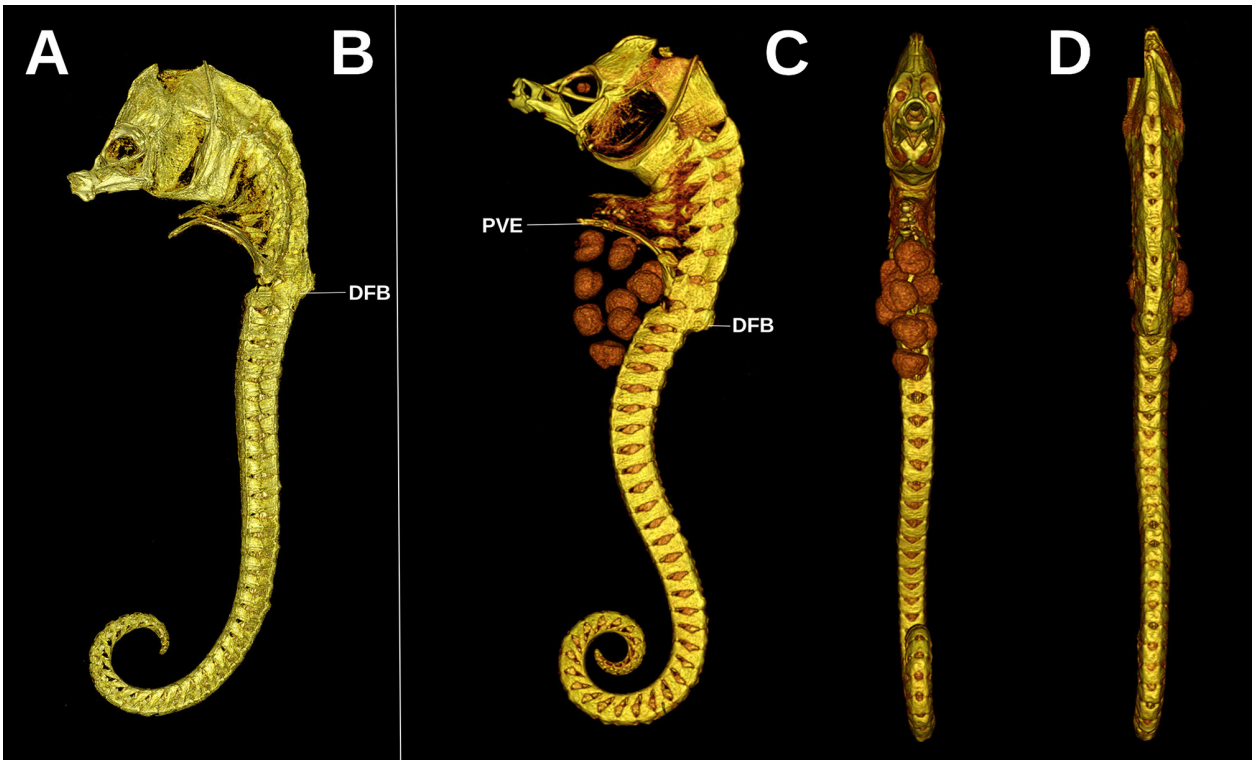

Figure 5. Micro-computed tomography (CT) scans of the skeletons of *Australyichthys minotaur*, male specimens. (A) CAS 13403, 33.7 mm SL, lateral view. (B–D) CSIRO H4464-01, 53.9 mm SL, lateral, anterolateral, and anterior views. Hydrated embryos (highlighted in red) are positioned beneath the posterior ventral elements (PVE) and median anal pterygiophore (MAP). Approximately nine embryos are visible within the brood pouch. Abbreviations: PVE = posterior ventral elements; MAP = median anal pterygiophore.

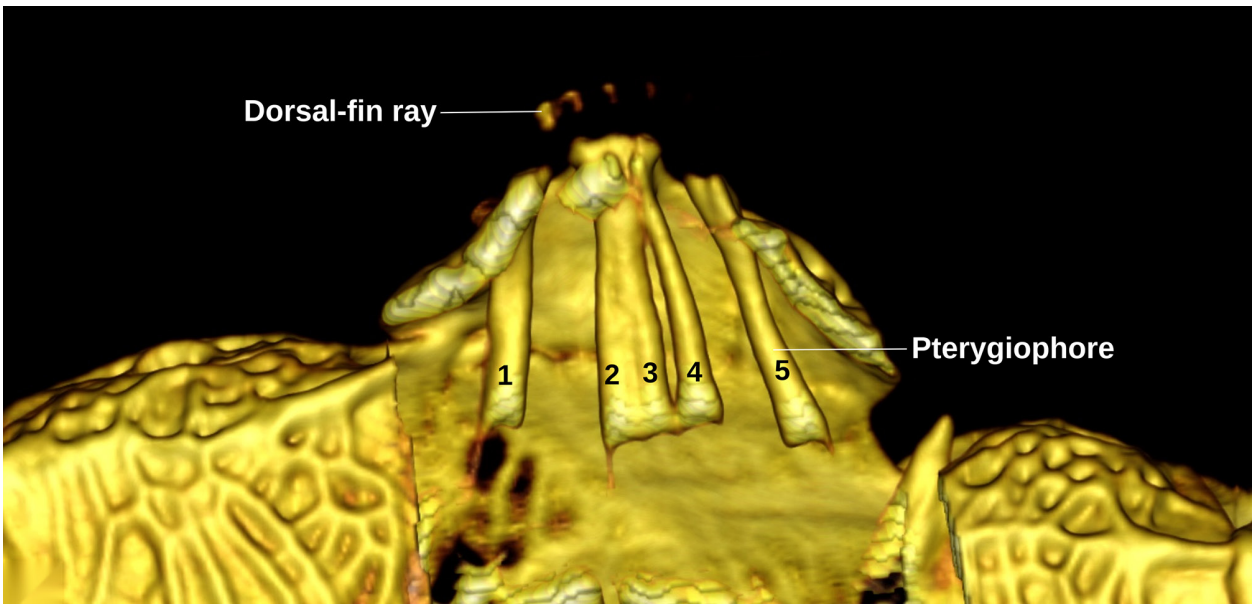

Figure 6. Micro-computed tomography (CT) cross-section through the dorsal fin base of *Australyichthys minotaur*, NMV A192, holotype, male, 48.7 mm SL, showing five robust pterygiophores supporting seven dorsal fin rays. The dorsal fin base is positioned entirely on the first tail ring. This configuration is unique to *A. minotaur* within the genus; both *A. paradoxus* and *A. aegis* lack the dorsal fin and all supporting skeletal elements.

shallow mound, an extremely deep "neck" only slightly shallower than head depth, and absence of inferior and median ventral trunk ridges. Gomon (1997) also noted a dorsal fin with seven rays and low pectoral and anal fin ray counts; these meristic values are corroborated by CT imaging (Figs. 2, 4–6). The absence of ventral ridges reflects the derived plate configuration diagnostic of *Australyichthys*, in which inferior trunk plates remain unfused along the ventral midline.

Gomon (1997:246) described "crescentic processes" projecting laterally from the ventral margin of the final trunk ring, suggesting they provided mechanical support to the posterior margin of the abdomen. CT reveals that these structures represent the posterior ventral elements (PVE) diagnostic of *Australyichthys*. In males, the PVE form unsegmented, curved ossifications (Figs. 2, 5); in females, they appear as broader, spatulate structures (Fig. 4). The crescentic morphology described by Gomon reflects the external contour of the combined AVE–PVE complex. The AVE in *A. minotaur* comprises four ossified units in males and two elongate ossified units in females; the PVE flank a centrally positioned MAP (Figs. 2, 4, 5). The dorsal fin comprises seven rays supported by five robust pterygiophores positioned entirely on the first tail ring (Fig. 6). Restriction of the dorsal fin base to the first tail ring contrasts with *Hippocampus*, in which the dorsal fin base extends across both trunk and tail rings (Figs. 13–15). Within *Australyichthys*, dorsal fin retention is restricted to *A. minotaur* whereas *A. paradoxus* and *A. aegis* lack the dorsal fin and all associated pterygiophores. Available material is insufficient to determine whether dorsal fin absence in these species represents shared or independent evolutionary loss.

Sexual dimorphism in *A. minotaur* occurs in the supraoccipital, AVE, and PVE. The supraoccipital is highly elevated in both sexes but more steeply angled in males, producing sex-specific head profiles (Figs. 2, 4). The AVE comprise four ossified elements in males and two elongate elements in females. The PVE in males consist of elongate, unsegmented ossifications closely associated with the MAP, forming a rigid support rostral and dorsal to the brood pouch; in females, the PVE are broad and spatulate and do not form a comparable supportive framework (Figs. 4, 5). CT imaging of male specimen CSIRO H4464-01 revealed approximately nine embryos within the brood pouch (Fig. 5), providing the first direct visualization of male brooding in this species. The posterior abdominal expansion emphasized by Gomon (1997) corresponds to the PVE–MAP complex, linking external abdominal morphology to underlying ventral skeletal structure and reproductive function.

All examined type and non-type material conforms to the meristic ranges reported by Gomon (1997) and Foster and Gomon (2010): trunk rings 8; tail rings 38–42. The documented depth range of 64–124 m places the species consistently within the temperate mesophotic zone.

Coloration in preservative. Coloration in life is unknown but is presumed to resemble that of the freshly preserved state. In the freshly preserved specimen, the head and dorsal region are pale orange to ochre, mottled with irregular, diffuse brown speckling, most concentrated along the snout and dorsum. The orbit is darkly pigmented and encircled by a faint translucent margin. The trunk is slightly deeper in hue, exhibiting a reticulated pattern of fine brownish-orange markings over a lighter orange-tan background. The lateral trunk surface, particularly the enlarged trunk area, is semi-translucent with a subtle marbled pattern. The dorsal fin is hyaline with a pale base; the pectoral fin is similarly translucent with faint orange pigmentation along the rays. The tail narrows posteriorly, maintaining a uniform basal orange-brown coloration with fine reticulations that become more linear and vermiform toward the tip. The ventral surface and underside of the tail are paler, and the distal tip terminates in a tightly coiled, slightly lighter-toned prehensile tail.

Distribution and habitat. Australyichthys minotaur is known from southeastern Australian waters and is currently confirmed from only three localities in New South Wales and Victoria (Fig. 11). The holotype (NMV A192) was collected off Eden, New South Wales, at depths of 64–73 m using a Danish seine trawl (Gomon, 1997). Paratypes include two females: AMS IA.3509 collected by trawl off the New South Wales coast, and AMS IA.3560 collected 13 km east of Eden at depths of 91.5–109.8 m (Gomon, 1997). Several non-type specimens have also been collected off Eden, suggesting that this region may represent suitable habitat for the species. An additional juvenile specimen (NMV A14161), not examined in the present study, was collected from Bass Strait, 38 km southwest of Cape Paterson, Victoria, at a depth of 70 m on fine sand substrate, using the RV Tangaroa on 12 November 1981. Collection data indicate an association with fine sandy habitats for at least one specimen. Anecdotal records suggest the species was encountered during environmental monitoring surveys off Wollongong, New South Wales (Gomon, 1997); however, examination of the original records suggests uncertainty in the identification of the observed specimens, which were considered more likely to represent juvenile *Hippocampus abdominalis*. Given the distinct morphology of *A. minotaur*, it is likely the species would have been clearly recognized if present.

Australyichthys paradoxus
(Foster & Gomon, 2010)
Short, Foster & Gomon, comb. nov.

(Figs. 7–8)

Common name: paradoxical sea Muppet.

Hippocampus paradoxus Foster & Gomon, 2010: 61–68, Figs. 1–4; Lourie et al., 2016: 34–35 (part). Holotype. SAMA F10490, female, 64.6 mm SL; Australia, Western Australia, SW of Esperance, Station GAB 108, 102 m depth, approximately 34.48°S, 121.53°E, 26 July 1995, collected by S. Hageman, P. Bock, and Y. Bone.

Diagnosis. Australyichthys paradoxus is distinguished from congeners by mid-dorsal dermal lobes broad, square-shaped, arranged along trunk and tail—two on trunk (first low, spanning trunk rings 1–3; second larger, spanning trunk rings 7–8), ten on tail (first spanning tail rings 3–5, subsequent lobes progressively smaller, posteriormost reduced to small tubercle); dorsal fin and all associated pterygiophores absent. The head is large and fleshy, with a short snout. The supraoccipital is elevated and anteriorly inclined. The anterior nuchal plate is reduced and free-floating. The first vertebra has a bifurcated anterior margin. The cleithrum is dorsally expanded, continuous, and extremely robust. The superior trunk ridges are elevated on rings 1–3, and the inferior trunk plates are unfused along the ventral midline. The ventral trunk region bears the AVE–PVE–MAP complex diagnostic of the genus. The AVE are paired, each a multisegmented series of five overlapping ossified units derived from the inferior plates of trunk rings 3–6. The PVE are paired, broad, spatulate ossifications associated with the last trunk ring, flanking a centrally positioned MAP. The species is known only from the female holotype, in which the hydrated oocytes are positioned within the abdominal cavity between the AVE and PVE. The trunk rings number 8, the tail rings 41, the pectoral-fin rays 11, and the anal-fin rays 4.

Coloration in preservative. Coloration in life is unknown. In preservative, the body is pale yellow-cream, diffusely speckled with minute brown chromatophores. Nuchal tubercles are densely pigmented with fine brown dots. A series of faint brown spots, some enclosing pale centers, extends along the dorsal midline from trunk rings 3 to 6.

Distribution and habitat. The species is only known from its type locality near Esperance, Western Australia, on the extreme western margin of the Great Australian Bight (Fig. 11). The holotype of *A. paradoxus* was collected from

Figure 7. *Australyichthys paradoxus*, SAMA F10490, holotype, female, 64.6 mm SL, preserved, southwestern Australia, off Esperance, Western Australia. Lateral view showing externally unsegmented trunk and tail and multiple fleshy dorsal lobes distributed across trunk and tail.

the mid-continental shelf of the Great Australian Bight at a depth of 102 m, in an area targeted for its rich bryozoan assemblages (Foster and Gomon, 2010). This mesophotic habitat is characterized by high-energy wave conditions and substrates composed of rippled calcareous sand interspersed with structurally complex bryozoan- and sponge-stabilized "islands". The substrate includes a diverse assemblage of bryozoans, such as species in the genera *Adeona* and in the family Catenicellidae, alongside "lace corals" (Phidoloporidae) and sponges (James et al. 2001). Seafloor photographs from the collection region illustrate this complex and biodiverse habitat (James et al. 2001). The mid-continental shelf across the Great Australian Bight remains sparsely surveyed, and syngnathid records are rare across this extensive (>2,500 km) coastline. Consequently, the ecology, habitat associations, and broader distributional limits of *A. paradoxus* remain poorly understood (Foster and Gomon 2010).

Notes on biology. CT scans of the female holotype revealed a high concentration of discrete, circular, high-density objects distributed throughout the trunk cavity. These structures are interpreted as remnants of ingested prey, most likely unidentifiable crustacean fragments, their elevated density consistent with the presence of calcified exoskeletal material. These fragments are primarily concentrated anterior to the developing oocytes and adjacent to visceral organs. The presence of these prey remnants is consistent with ingestion of minute benthic or planktonic crustaceans, indicating that *A. paradoxus* may feed opportunistically on small invertebrates present within its mesophotic habitat.

Remarks. Australyichthys paradoxus is known only from the female holotype. The species was originally described as *Hippocampus paradoxus* based on its modified external morphology, including a soft, externally unsegmented trunk and tail, obscured ring boundaries, and prominent dorsal dermal lobes (Foster and Go-

mon 2010). The difficulty of placing this species within *Hippocampus* was noted given the absence of a dorsal fin and the presence of unusual ossified structures associated with the trunk (Foster and Gomon 2010; Gomon 1997). CT examination in the present study demonstrates that *A. paradoxus* conforms to the diagnostic characters of *Australyichthys*, supporting its reassignment.

Foster and Gomon (2010) provided a detailed description of the holotype based on external morphology, radiography, and CT imaging. They documented a prominent head (HL 15.2% SL) with axis approximately 90° to trunk axis; a particularly robust cleithrum making the head bulbous posteriorly; head deep (HD 85.7% HL), rising steeply from a short snout (SnL 25.5% HL) to a prominent supraoccipital; first nuchal plate prominent dorsally, of similar height to supraoccipital relative to the horizontal axis of the head and much higher than the second nuchal plate; coronet evident only in radiograph as diffuse ossification lying between supraoccipital and first nuchal plate, not in contact with supraoccipital; and gill openings narrowly separated at top of head just anterior to cleithrum. Foster and Gomon (2010) also described a fleshy ridge-like crest extending posteriorly from the supraoccipital between gill openings and over the first nuchal plate, noting this crest as the highest point on the head, and a blunt fleshy "neck spine" adorned with short

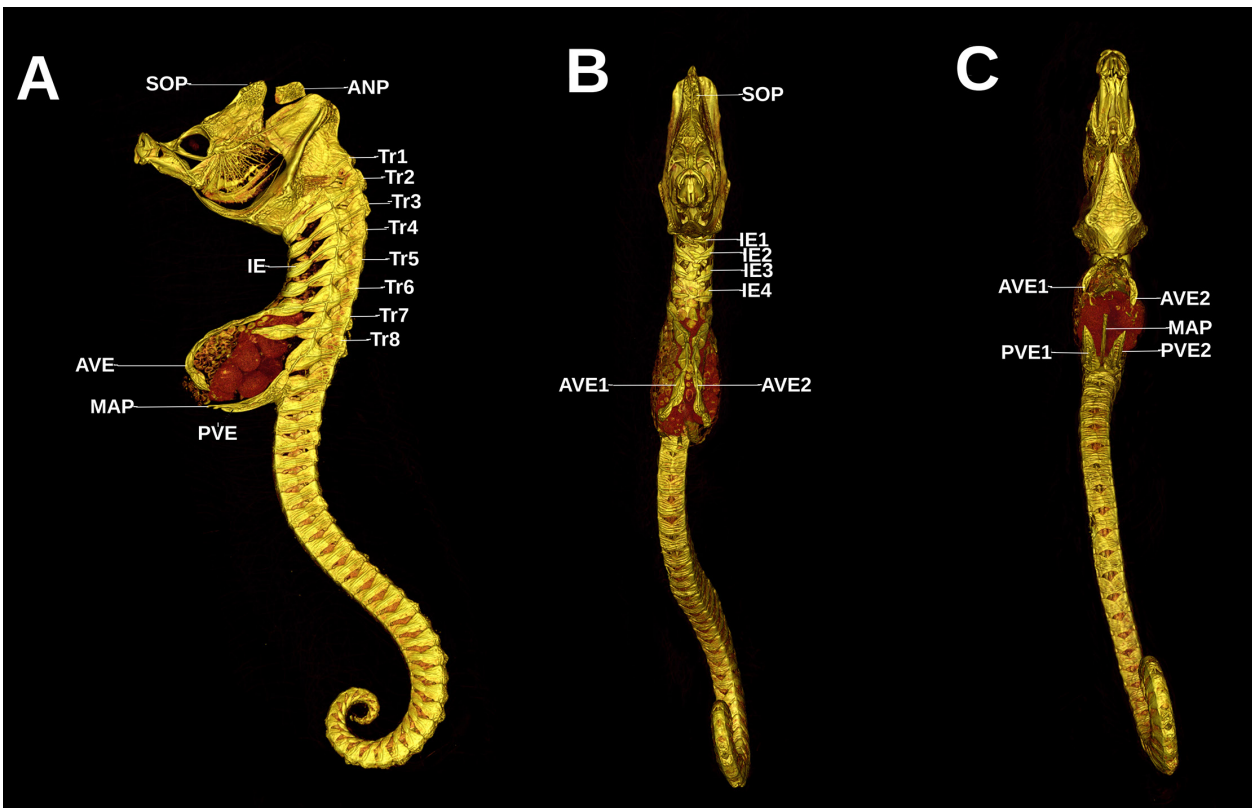

Figure 8. Micro-computed tomography (CT) scans of the skeleton of *Australyichthys paradoxus*, SAMA F10490, holotype, female, 64.6 mm SL. (A) Lateral view showing robust cleithrum, eight trunk rings, and forty-one tail rings. (B) Anterior view showing unfused inferior trunk plates and ventral support structure. (C) Dorsolateral view highlighting the proportionally long and slender posterior ventral elements (PVE) characteristic of the species. Views show the anterior ventral elements (AVE), posterior ventral elements (PVE), median anal pterygiophore (MAP), inferior trunk plates (IP), and trunk rings (Tr). Abbreviations: AVE = anterior ventral elements; PVE = posterior ventral elements; MAP = median anal pterygiophore; IP = inferior plate; Tr = trunk ring; ANP = anterior nuchal plate.

cirri at the intersection of the superior trunk ridge with trunk ring 1. CT in the present study reveals that this fleshy crest corresponds externally to the elevated superior trunk ridges on rings 1–3. The diffuse ossification interpreted by Foster and Gomon (2010) as a remnant coronet is here identified as a reduced, free-floating anterior nuchal plate that lacks the structural integration with the supraoccipital required to form a discrete coronet.

The orbit is surrounded by 9 conical papillae, with additional conical papillae distributed across the head, including a broad-based "nose spine" just anterior to the eyes, and smaller papillae on the snout, forehead, supraoccipital, operculum, around gill openings, and overlying the second nuchal plate (Foster and Gomon 2010). The dorsal surface is densely covered with microscopic papillae.

Mid-dorsal dermal lobes are well developed, broad, and square-shaped, arranged strictly along the dorsal midline: two on trunk (first low, spanning trunk rings 1–3; second larger, spanning trunk rings 7–8, resembling a dorsal fin but fleshy and without rays); ten on tail (first spanning tail rings 3–5, subsequent lobes fairly regularly spaced, each spanning about 2–2.5 rings, becoming progressively smaller and less distinctively shaped posteriorly, posteriormost reduced to small tubercle; second tail lobe considerably smaller than first and third). Pairs of small, fleshy, flange-like lateral outgrowths occur adjacent to inferior tail ridges ventral to the second and third tail lobes. The dorsal fin and all associated pterygiophores are absent.

Foster and Gomon (2010) described the osteology based on CT imaging, noting mostly complete but very light ossification dorsally; superior and lateral trunk ridges are clearly discernible but lateral trunk ridge is lost with ossification decreasing just prior to the tail; trunk ring 1 completely encircles the neck and is fused to the cleithrum; remaining thoracic rings (trunk rings 2–6) are almost encircling the trunk but are unfused ventrally, with ventral trunk ridge absent; and trunk ring 7 is similar but not encircling the body due to the expanded abdomen. These observations are consistent with CT-based interpretation in the present study of reduced ventral trunk ossification diagnostic of *Australyichthys*, in which discrete ventral ossifications (AVE, PVE, MAP) provide structural support rather than midline fusion of ventral plates. Foster and Gomon (2010) described "ossified ventral elements associated with last trunk ring (TrR8) scaffold-like, somewhat extended and strongly angled posteriorly, following contour of posterior surface of abdomen"; CT in the present study identifies these structures as the posterior ventral elements (PVE), which arise from the final trunk ring as broad, spatulate ossifications flanking the MAP (Fig. 8). Foster and Gomon (2010) also documented "segmented inferior trunk ridge remnants, originating from TrR6 ossified elements," which followed the contour of the abdomen, converging ventroposteriorly to run almost parallel adjacent to the ventral midline before diverging after trunk ring 7 and recurving dorsoposteriorly, terminating just anterior to the anus; CT in the present study identifies these structures as the anterior ventral elements (AVE), which originate from the inferior plates of trunk rings 3–6 and form overlapping ossifications beneath the abdominal cavity.

Foster and Gomon (2010: 64) noted an ossified element at the base of the second dorsal dermal lobe, initially interpreted as a possible remnant of dorsal fin pterygiophores before being reconsidered as a bony outgrowth of the superior trunk ridge. CT in the present study clarifies that this structure represents neither a retained dorsal fin pterygiophore nor an outgrowth of the superior trunk ridge. Its apparent position reflects lateral overlap between the dorsal dermal lobe and the ventral ossification complex, particularly the MAP. Three-dimensional reconstructions demonstrate that the element originates ventrally and forms part of the AVE–PVE–MAP complex, resolving the ambiguity noted by Foster and Gomon (2010) and confirming complete absence of dorsal fin supports.

Comparison with A. minotaur. Foster and Gomon (2010) compared *H. paradoxus* with *H. minotaur*, documenting several differences: the cleithrum of *A. paradoxus* is much more robust and the first nuchal plate more dorsally prominent, with a height similar to the supraoccipital; in *A. minotaur*, the supraoccipital is tallest and the head lacks the fleshy crest, tapering instead into a deeper anterior trunk. *Australyichthys paradoxus* possesses 9 circumocular papillae and additional conical papillae distributed across the head; *A. minotaur* lacks circumocular papillae. Mid-dorsal dermal lobes in *A. paradoxus* are well developed, broad, and square-shaped; in *A. minotaur*, dermal lobes are reduced to minute tubercular swellings or absent. Foster and Gomon (2010) noted that thoracic rings (trunk rings 2–6) are retained ventrally, at least in part, in *A. paradoxus*, whereas *A. minotaur* appears to have lost them ventrally. Radiography of the female *H. minotaur* paratype (AMS IA.3509) revealed "extended TrR8 ossified elements" and "indications of inferior trunk ridge remnants girdling the anterior of the abdomen"; these observations correspond to the PVE and AVE respectively, indicating that Foster and Gomon (2010) had identified components of the ventral support complex in both species, although the homology and diagnostic significance of these structures was not recognized at the time.

CT in the present study reveals additional osteological differences. The superior trunk ridges are elevated on rings 1–3 in *A. paradoxus* but are not elevated in *A. minotaur* (Figs. 3–6, 8). The AVE are expressed as paired multisegmented series in *A. paradoxus* but as a single median multisegmented series in *A. minotaur* (Figs. 2, 4, 5, 8). The dorsal fin and all associated pterygiophores are absent in *A. paradoxus*; *A. minotaur* retains a dorsal fin with seven rays supported by five pterygiophores positioned entirely on the first tail ring (Fig. 6).

The holotype contains 11 hydrated oocytes, each approximately 2 mm in diameter, positioned within the abdominal cavity between the AVE and PVE, consistent with females of *A. minotaur*. Because *A. paradoxus* is known only from a single female specimen, sex-specific variation in ventral trunk morphology cannot be assessed.

Australyichthys aegis Short, Foster & Gomon, sp. nov.

(Figs. 9–10)

Common name: helmethead sea Muppet.

Holotype. SAMA F14993, male, 56.0 mm SL; Australia, South Australia, entrance to Spencer Gulf, Gambier Islands, approximately 50 m depth, 35.20°S, 136.27°E, 11 February 2006; collected by dredge deployed to sample brachiopods during the Waterhouse Club Expedition – Verco 2006.

Paratypes. None; *Australyichthys aegis* is known only from the holotype, which is the sole specimen available.

Diagnosis. Australyichthys aegis is distinguished from congeners by mid-dorsal dermal lobes that are sharply triangular, laterally compressed, arranged singly along dorsal midline of trunk and tail—one large lobe spans trunk rings 3–8, with six additional lobes on tail progressively decreasing in size; dorsal fin and all associated pterygiophores are absent. The head is extremely large and dome-shaped, with a steep dorsal profile. The supraoccipital is highly elevated and angled anteroposteriorly. The anterior nuchal plate is sharply tapered and rugose, firmly embedded within the bifurcated anterior margin of the first vertebra (not free-floating as in congeners), and does not articulate with the supraoccipital. The first vertebra has an elevated, irregular dorsoposterior margin that projects posteriorly. The cleithrum is robust and continuous. The first trunk ring bears a distinct, elevated, rugose bony crest immediately posterior to the cleithrum. All superior trunk ridges are elevated, including that of the anteriormost tail ring; the superior and lateral trunk plates are fused; and the inferior trunk plates are unfused along the ventral midline. The ventral trunk region bears the AVE–PVE–MAP complex diag-

nostic of the genus. The AVE are paired, each a multisegmented series of four partially overlapping ossified units with the terminal segment recurved ventrally, originating from the inferior plates of trunk ring 6. The PVE are paired, broad, and spatulate, fused proximally and diverging distally to partially enclose the MAP between their separated termini, originating from trunk ring 8. The inferior plates of trunk rings 1–6 are longitudinally compacted, those of rings 1–4 overlapping without interdigitating, whereas the inferior plates of trunk rings 7–8 are oriented laterally and do not overlap at the ventral midline. The trunk rings number 8 and the tail rings 38. The pectoral-fin rays number 10, and the anal fin is reduced or absent.

Description. Body shape illustrated in Figs. 9–10; morphometric and meristic data in Table 2. The body is extremely compressed and fleshy, lack-

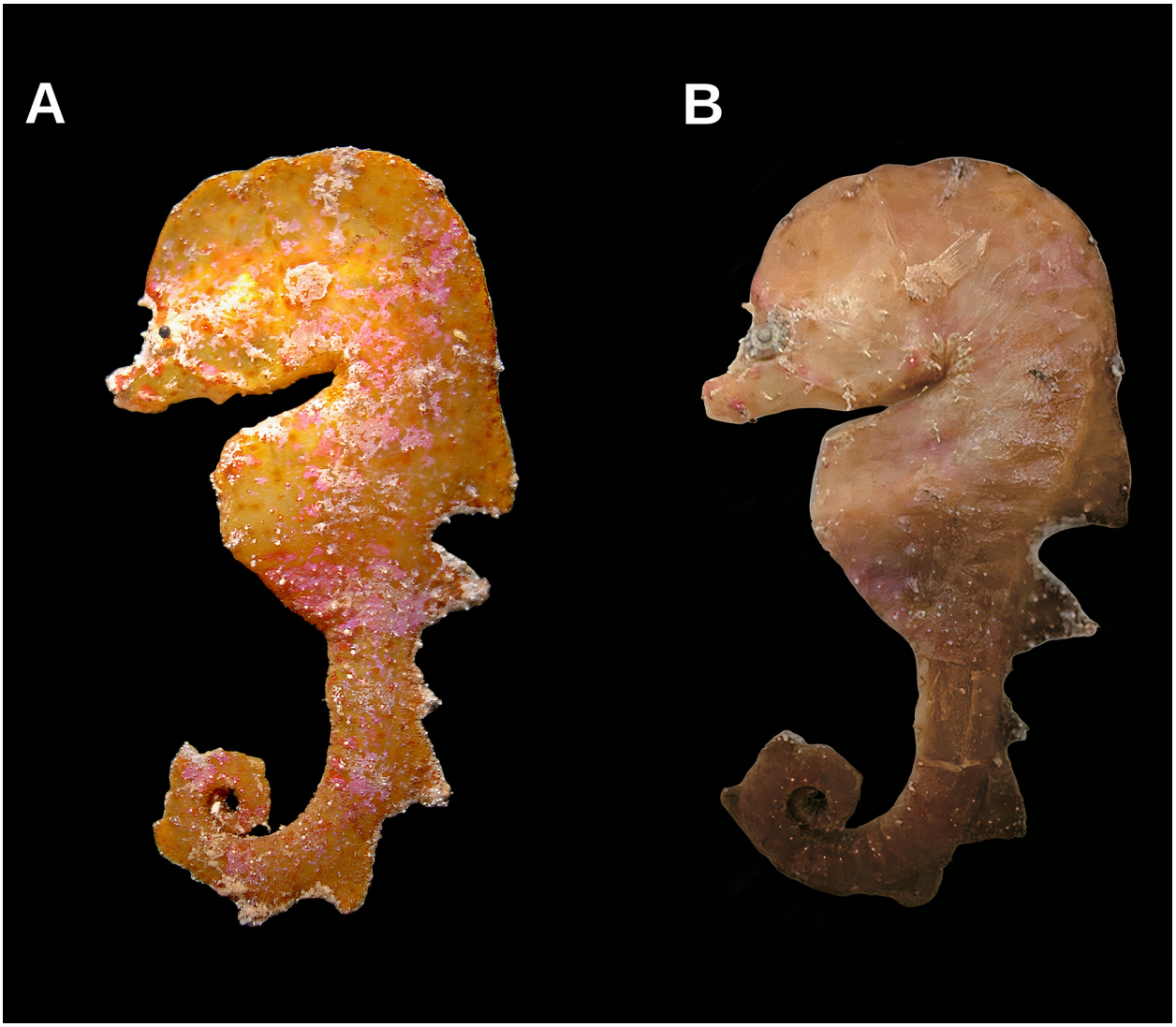

Figure 9. *Australyichthys aegis*, SAMA F14993, holotype, male, 56.0 mm SL, entrance to Spencer Gulf, Gambier Islands, South Australia. (A) Freshly collected specimen showing vivid orange to pink-orange coloration with irregularly distributed patches and blotches of pink, white, and pale yellow. (B) Preserved specimen showing faded pale yellow-brown base coloration with scattered white and silvery speckles. Note the sharply triangular, laterally compressed dorsal dermal lobes arranged as a single large trunk lobe followed by six progressively smaller tail lobes.

ing visible bony segmentation; the head–trunk junction is without exaggerated constriction; and the head axis is approximately 90° to the trunk axis. The abdomen is protuberant and barrel-shaped in lateral view. The head is extremely large and dome-shaped, with a steep dorsal profile (HL 17.5% SL; HD 88.8% HL), and the snout is short and blunt (SnL 25.8% HL). The gill openings are positioned at the highest point of the cleithrum, separated by a fleshy crest extending along the dorsum; this crest corresponds externally to the elevated superior trunk ridges, a feature shared with *A. paradoxus* but absent in *A. minotaur*. The body lacks dermal filaments, spines, or ornamentation. The pectoral fin has 10 rays. The dorsal fin is absent; CT confirms the complete absence of dorsal-fin rays, pterygiophores, and neural-spine modifications (Fig. 10). The anal fin is not visible externally and is presumed reduced or absent. The trunk is short and compact, comprising 8 rings. The tail is elongate and prehensile, comprising 38 rings; the caudal fin is absent.

Dermal lobes arranged along the dorsal midline of trunk and tail (Fig. 9), sharply triangular and laterally compressed. A long, low, fleshy ridge spans trunk rings 2–4, distinct from the dermal lobes. A single large triangular lobe spans trunk rings 3–8. Six additional lobes occur on the tail: first originating on tail ring 1, spanning four rings; second spanning two rings; third spanning four rings; fourth spanning three rings; fifth and sixth each spanning two rings.

CT reveals a markedly elevated supraoccipital angled anteroposteriorly (Fig. 10A–B). Anterior nuchal plate sharply tapered, rugose, firmly embedded within the bifurcated anterior margin of the first vertebra, not free-floating as in congeners (Fig. 10D). Dorsoposterior margin of first vertebra elevated, craggy, projecting

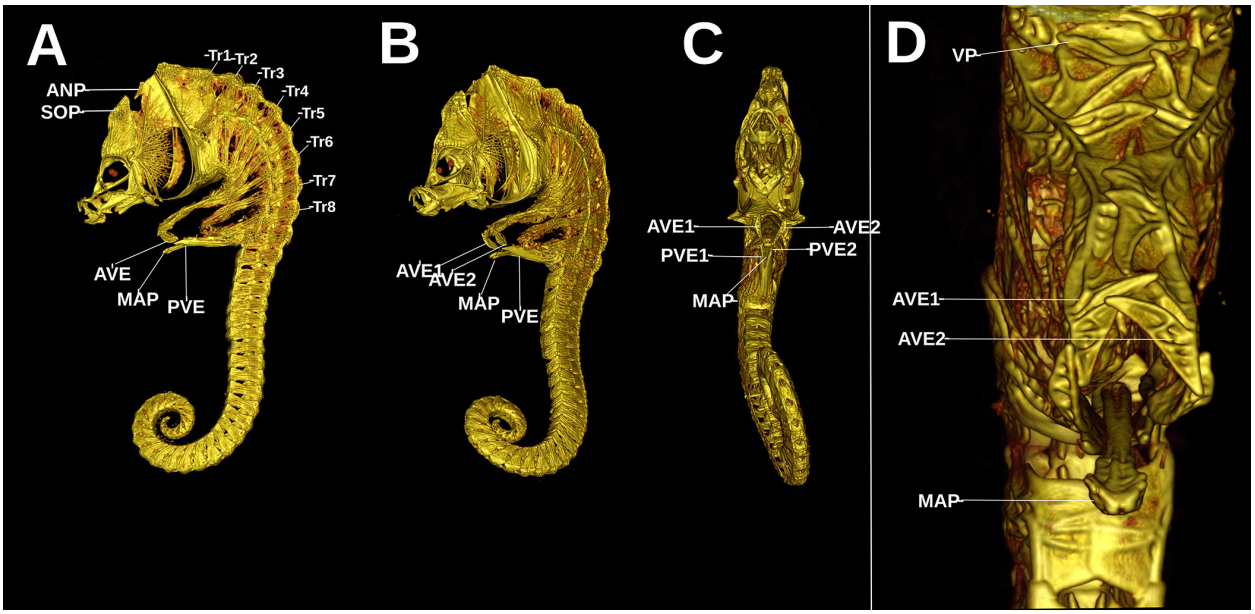

Figure 10. Micro-computed tomography (CT) scans of the skeleton of *Australyichthys aegis*, SAMA F14993, holotype, male, 56.0 mm SL. (A–C) Lateral, anterolateral, and anterior views showing the anterior ventral elements (AVE), posterior ventral elements (PVE), median anal pterygiophore (MAP), and trunk rings (Tr). Note the fused spatulate PVE enclosing the MAP in anterior view (C). (D) Anterior trunk region showing the multi-segmented anterior ventral elements (AVE), each comprising four partially overlapping segments with the terminal segment recurved ventrally, and the centrally positioned median anal pterygiophore (MAP). The anterior nuchal plate (ANP) is firmly embedded within the bifurcated anterior margin of the first vertebra. Abbreviations: AVE = anterior ventral elements; PVE = posterior ventral elements; MAP = median anal pterygiophore; ANP = anterior nuchal plate; Tr = trunk rings.

Table 2. Select morphometric measurements and meristic counts for species of *Australyichthys* examined in this study. Measurements are expressed as percentages of standard length (SL) or head length (HL), as indicated. Abbreviations: SL = standard length; HL = head length; TrL = trunk length; TaL = tail length; CH = head depth at cleithrum; HD = maximum head depth; SnL = snout length; DF = dorsal fin rays; PF = pectoral fin rays; AF = anal fin rays; TrR = trunk rings; TaR = tail rings. Institutional abbreviations follow Sabaj (2020). Sex is indicated.

Measurement	***A. minotaur***	***A. minotaur***	***A. minotaur***	***A. minotaur***	***A. minotaur***	***A. paradoxus***	***A. aegis***
Voucher	NMV A192	AMS IA.3509	AMS IA.3560	CSIRO 4464-01	CAS 13403	SAMA F10490	SAMA F14993
Type status	Holotype	Paratype	Paratype	Non-type	Non-type	Holotype	Holotype
SL (mm)	48.7	42.2	52.6	53.9	33.7	64.6	56.0
Sex	Male	Female	Female	Male	Male	Female	Male
% SL							
HL	14.4	16.0	15.9	14.9	15.1	15.2	17.5
TrL	16.4	20.4	18.2	17.8	16.9	22.9	22.9
TaL	69.2	64.0	65.9	67.3	68.0	61.9	59.6
% HL							
CH	69.2	59.7	67.0	61.3	64.7	50	59
HD	91.2	79.4	85.7	85.0	76.5	85.7	88.8
SnL	28.5	30.9	28.7	21.3	25.4	25.5	25.8
Counts							
Trunk rings	8	8	8	8	8	8	8
Tail rings	41	42	38	41	40	41	38
DF	7	7	7	7	7	–	–
PF	11	11	11	11	11	11	10

posteriorly beyond the adjacent dorsal margin. CT reveals a markedly elevated supraoccipital angled anteroposteriorly (Fig. 10A–B). The anterior nuchal plate is sharply tapered and rugose, firmly embedded within the bifurcated anterior margin of the first vertebra, and is not free-floating as in congeners (Fig. 10D). The dorsoposterior margin of the first vertebra is elevated and craggy, projecting posteriorly beyond the adjacent dorsal margin. The cleithrum is robust and continuous, appearing discontinuous where the cleithral arm does not extend completely over the first vertebra. All superior trunk ridges are elevated, and the anteriormost tail ring also bears an elevated superior ridge. The superior and lateral trunk plates are fused, forming a continuous exoskeletal frame, whereas the inferior plates are unfused along the ventral midline (Fig. 10A). The inferior plates of trunk rings 1–6 are longitudinally compacted, and those of trunk rings 1–4 overlap without interdigitating (Fig. 10B). The inferior plates of trunk rings 7–8 are oriented laterally and do not overlap at the ventral midline. The inferior plates of trunk ring 6 are connected ventrally to a large unpaired plate (Fig. 10D).

The ventral trunk bears the AVE–PVE–MAP complex diagnostic of the genus (Fig. 10A–D). The AVE originate from the inferior plates of trunk ring 6 as paired, multisegmented elements (Fig. 10A–B, D); each element comprises four partially overlapping ossified units, the terminal unit recurved ventrally. The PVE originate from trunk ring 8 as a pair of broad, spatulate ossifications, fused proximally and diverging distally to partially enclose a centrally positioned, cylindrical MAP between their separated termini (Fig. 10C–D). This configuration differs from *A. minotaur* and *A. paradoxus*, in which the PVE remain paired and unfused. In anterior view, the overlapping AVE and

fused PVE form a reinforced, tunnel-like configuration encasing the MAP within a semi-enclosed channel.

Remarks. Australyichthys aegis is known only from the male holotype (SAMA F14993), the sole ethanol-preserved specimen of the genus, enabling extraction of high-quality DNA and providing molecular confirmation of the placement of *Australyichthys* within Haliichthyini (Fig. 12). Because no female is known, sex-specific variation in ventral trunk morphology and dermal lobe development cannot be evaluated.

Externally, *A. aegis* shares the enlarged, fleshy head, soft externally unsegmented trunk and tail, and absence of spination diagnostic of the genus. The species differs from congeners in dermal lobe morphology (Fig. 9): lobes in *A. aegis* are sharply triangular and laterally compressed, arranged singly along the dorsal midline; in *A. paradoxus*, lobes are broad and square-shaped; in *A. minotaur*, lobes are reduced or absent. A fleshy crest extends along the dorsum from the supraoccipital, a feature that is shared with *A. paradoxus* but absent in *A. minotaur*; CT reveals that this crest corresponds externally to the elevated superior trunk ridges. The dorsal fin and all associated pterygiophores are absent, as in *A. paradoxus*; *A. minotaur* retains a dorsal fin with seven rays supported by five pterygiophores.

Neurocranial and trunk osteology also differ among species. The anterior nuchal plate (ANP) in *A. aegis* is sharply tapered, rugose, and firmly embedded within the bifurcated anterior margin of the first vertebra (Fig. 10D), not free-floating as in *A. minotaur* and *A. paradoxus* (Figs. 3–6, 8). The ANP is proportionally smallest in *A. aegis*, intermediate in *A. minotaur*, and largest in *A. paradoxus*. The first vertebra in *A. aegis* exhibits an elevated, craggy dorsoposterior margin, and a distinct, elevated, rugose bony crest occurs on the first trunk ring immediately posterior to the cleithrum (Fig. 10B); these features are absent or less developed in congeners. The supraoccipital is highly elevated in all species; in *A. minotaur*, angulation is sexually dimorphic (more steeply inclined in males), but whether similar dimorphism occurs in *A. aegis* or *A. paradoxus* cannot be assessed from available material. Superior trunk ridges are elevated on all trunk rings in *A. aegis*, including the anteriormost tail ring (Fig. 10A); in *A. paradoxus*, elevation is restricted to trunk rings 1–3; in *A. minotaur*, superior trunk ridges are not elevated (Figs. 3–6, 8).

The ventral trunk skeleton of *A. aegis* exhibits the most derived configuration of the AVE–PVE–MAP complex within *Australyichthys* (Fig. 10). The AVE are paired and multisegmented, originating from the inferior plates of trunk ring 6; each comprises four partially overlapping ossified units, the terminal unit recurved ventrally. In *A. paradoxus*, the AVE are paired with five segments per element (Fig. 8) and in *A. minotaur*, the AVE is expressed as a single median multisegmented series (Figs. 3–6). The PVE in *A. aegis* arise from trunk ring 8 as broad, spatulate ossifications, fused proximally and diverging distally to partially enclose the MAP between their separated termini (Fig. 10C–D). In *A. minotaur* and *A. paradoxus*, the PVE remain paired and unfused. In anterior view, the overlapping AVE and fused PVE of *A. aegis* form a reinforced, tunnel-like configuration encasing the MAP within a semi-enclosed channel; this configuration is not observed in congeners.

In *A. minotaur*, PVE morphology is sexually dimorphic: males bear elongate, rod-like PVE with blunt distal termini, whereas females bear broad, spatulate PVE whose distal ends fuse to the MAP. The fused PVE configuration in the male holotype of *A. aegis* differs from males of *A. minotaur* and may represent species-level variation or an alternative male PVE morphology; resolution requires additional specimens.

The holotype of *A. aegis* (56.0 mm SL) is intermediate in size between the smallest known *A. minotaur* specimen (33.7 mm SL) and the holotype of *A. paradoxus* (64.6 mm SL); however, size ranges across the genus are largely overlapping (33.7–64.6 mm SL) and size compari-

sons are constrained by limited material. The holotype was collected at approximately 50 m depth, shallower than the 64–124 m range documented for *A. minotaur* and the 102 m depth for *A. paradoxus*, although all three species occur within the temperate mesophotic zone. The type locality in Spencer Gulf, South Australia, is geographically intermediate between southeastern Australia (*A. minotaur*) and the western Great Australian Bight (*A. paradoxus*), spanning approximately 2,500 km of southern Australian coastline.

Coloration. In life, the body is vivid orange to pink-orange, overlaid with irregularly distributed patches and blotches of pink, white, and pale yellow. Fine white chromatophores and pale pink pigment granules are distributed across the integument, with highest density over the head, nape, and anterior trunk, collectively producing a mottled appearance. Finer speckling of pink chromatophores traces subtle contours of the dermal surface, enhancing camouflage. Along the dorsal midline of the trunk and tail, the dermal lobes exhibit modest soft-tissue growth, contributing to an irregular outline and further disrupting the body's silhouette. Pigmentation fades along the lower flanks and is markedly reduced on the ventral surfaces, where pale or translucent areas contrast with the denser dorsolateral pigmentation. The prehensile tail retains the mottled pattern, with the curled tip tinged in pink and white. In ethanol, body coloration fades to a pale yellow-brown base, with scattered white and silvery speckles across the head, trunk, and tail.

Distribution and habitat. Australyichthys aegis is known only from its type locality, where the holotype was collected from approximately 50 m depth in the waters between the Gambier Islands and Neptune Islands, near the entrance to Spencer Gulf, South Australia (Fig. 11), during the Waterhouse Club Expedition – Verco 2006, a survey conducted by the Waterhouse Club in affiliation with the South Australian Museum. This expedition ranged from the Sir Joseph Banks Group Archipelago to southwest of the Gambier Islands and primarily targeted marine invertebrates, such as sponges and soft corals. The Gambier and Neptune Islands form a small archipelago situated between the southern tips of the Eyre and Yorke Peninsulas, within the Eyre Yorke Block bioregion, which spans the mid-southern part of South Australia (Department for Environment and Heritage [DEH] 2009; Department of Environment, Water and Natural Resources [DEWNR] 2012a, 2012b). The specific habitat of the holotype remains unknown owing to the limited locality data recorded during this non-scientific expedition. However, the surrounding Gambier Islands Group Marine Park includes diverse marine habitats, particularly in the southern and southwestern areas of the Gambier Islands. Reefs around the islands extend from the intertidal zone into deep water, exceeding 50 m in depth on its southwestern side (DEH 2009; DEWNR 2012a, 2012b). Large portions of the seafloor in the Eyre Yorke Block bioregion remain unsurveyed (DEH 2008), and the habitat preferences and ecological role of *A. aegis* are correspondingly undocumented.

Etymology. The specific epithet *aegis* (Latinized from the Greek *aigis*) refers to the protective shield or breastplate in Greek mythology. The name refers to the species' prominent domed head, recalling the protective strength of the *aegis*, and follows the mythologically derived epithets of its congeners. Treated as a noun in apposition.

Phylogenomic reclassification

The phylogenomic dataset comprised twenty-three syngnathid species (the 22 comparator taxa in Table 1 plus *Australyichthys aegis*) and 271 loci. Maximum Likelihood (IQ-TREE) and weighted ASTRAL species-tree analyses produced congruent topologies rooted by the outgroup *Doryrhamphus excisus* (Fig. 12). *Aus-*

tralyichthys is recovered as phylogenetically excluded from Hippocampini *sensu* Stiller et al. (2022) (UFBoot = 100; LPP = 1.0), a tribe defined to include the genus *Hippocampus* as well as the pipefishes *Halicampus macrorhynchus* and *H. punctatus*. Instead, the new genus is nested within Haliichthyini, a tribe comprising a diverse assemblage of Indo-Pacific pipefishes together with the Pacific pygmy pipehorses (*Idiotropiscis*, *Acentronura*, and *Cylix*). Within Haliichthyini, *Australyichthys* is recovered as the sister lineage (UFBoot = 100; LPP = 1.0) to a clade containing *Filicampus tigris*, *Trachyrhamphus*, *Halicampus grayi*, and *Haliichthys taeniophorus*. Collectively, Haliichthyini is recovered with strong statistical support as the sister group to Hippocampini, which comprises *Hippocampus* and closely allied pipefishes. Because genomic data could be obtained only from the ethanol-preserved holotype of *A. aegis*, the molecular placement of *Australyichthys* rests on that single species; referral of *A. minotaur* and *A. paradoxus* to the genus is based on the shared osteological synapomorphies documented above rather than on sequence data.

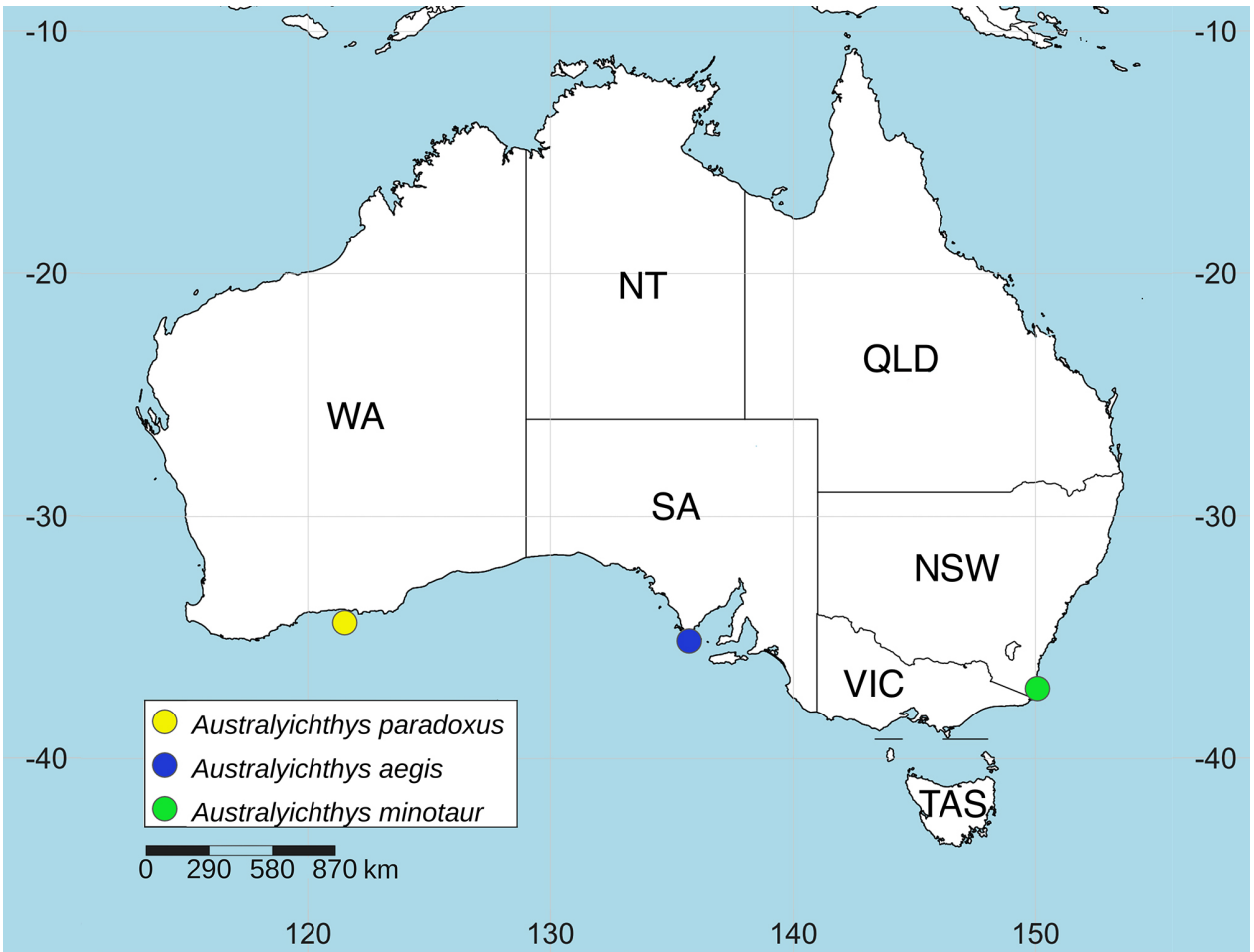

Figure 11. Map of the southern coast of Australia showing the type localities (indicated by colored circles) of the three species of *Australyichthys*. Green circles indicate collection sites for *A. minotaur* (off Eden, New South Wales, and Bass Strait, Victoria); at the New South Wales site, the symbol represents several specimens collected within a small area off Eden; yellow circle indicates the type locality for *A. paradoxus* (off Esperance, Western Australia, Great Australian Bight); blue circle indicates the type locality for *A. aegis* (Gambier Islands, entrance to Spencer Gulf, South Australia). All specimens were collected from mesophotic depths (50–124 m) as trawl bycatch. Map generated using SimpleMappr (Shorthouse, 2010).

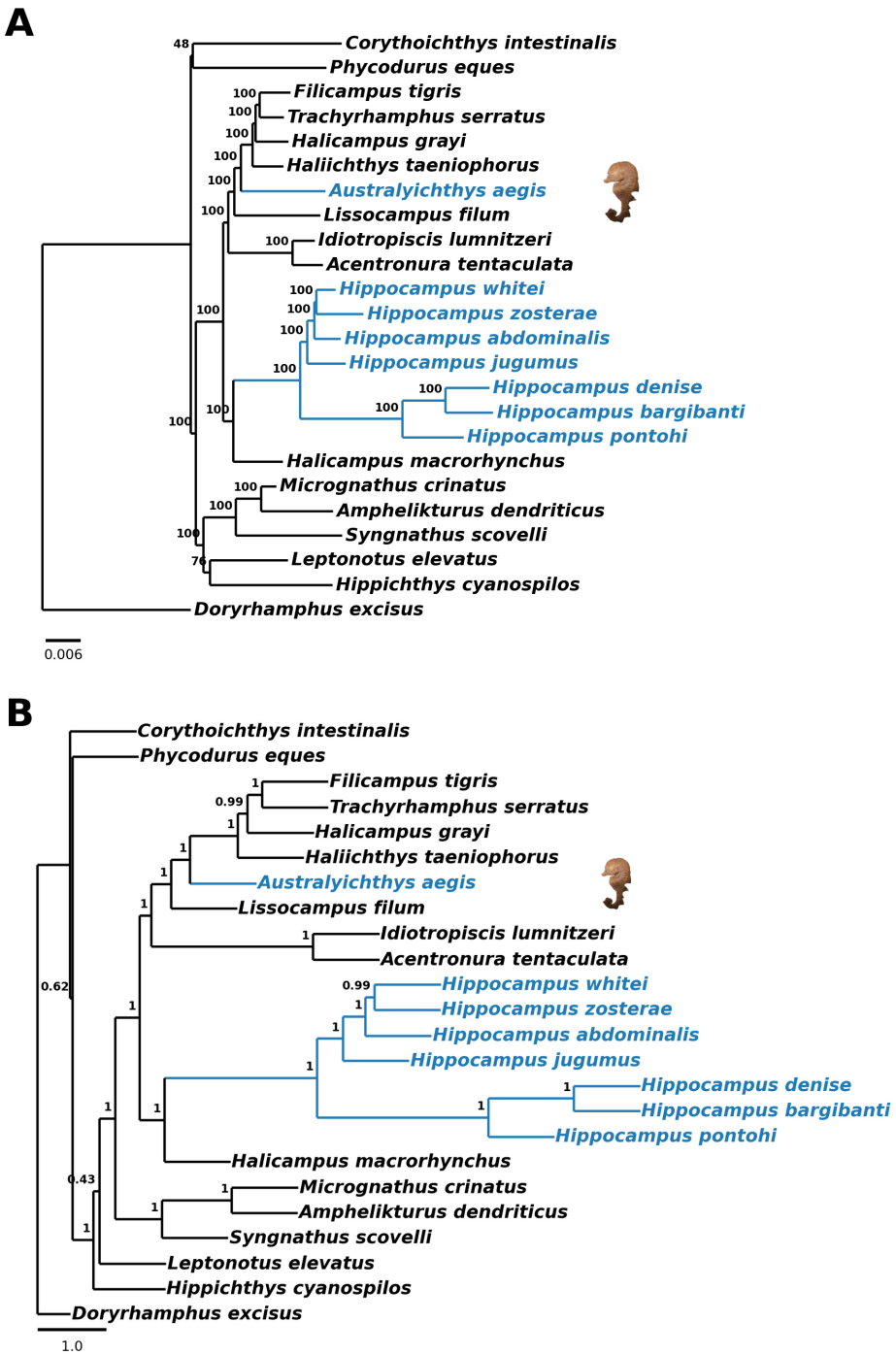

Figure 12. Concatenated-alignment Maximum Likelihood (IQ-TREE) phylogenetic tree with ultrafast bootstrap (UFBoot) support values ranging from 0 to 100 (A) and weighted ASTRAL (wASTRAL) species tree with local posterior probability support values ranging from 0 to 1 (B). Branch lengths were inferred from the concatenated Maximum Likelihood (IQ-TREE) analysis; terminal branch lengths are not inferred by wASTRAL and are displayed uniformly for visualization purposes. Both topologies are rooted on the outgroup species *Doryrhamphus excisus*, a member of the tail brooding syngnathids. Branches colored blue represent *A. aegis* and members of *Hippocampus*. *Australyichthys* was previously classified within *Hippocampus* but is recovered outside the monophyletic *Hippocampus* clade (Clade VII, Hippocampini) in both phylogenetic analyses, supporting its reassignment. *Australyichthys* is resolved within Haliichthyini, sister to *Filicampus*, *Trachyrhamphus*, *Halicampus*, and *Haliichthys*. Images of *Australyichthys aegis* holotype shown at right.

Phylogenetic position and morphological convergence

Phylogenomic analysis places *Australyichthys* within Haliichthyini, a diverse clade originally identified in molecular phylogenies by Hamilton et al. (2017) and Stiller et al. (2022). The genus is recovered within an Indo-Pacific assemblage comprising *Filicampus tigris*, *Trachyrhamphus*, *Halicampus grayi*, *Haliichthys taeniophorus*, *Lissocampus*, and the Indo-Pacific pygmy pipehorses *Idiotropiscis* and *Acentronura*. This placement, distinct from Hippocampini *sensu* Stiller et al. (2022), demonstrates that external seahorse-like morphology does not indicate close evolutionary relationship with *Hippocampus*. The shared occurrence of a ventrally angled head, prehensile tail, and fully enclosed brood pouch in *Australyichthys*, pygmy pipehorses, and *Hippocampus* represents repeated emergence of similar morphology across phylogenetically disparate lineages. This character combination is not restricted to Indo-Pacific taxa but also occurs in the Western Atlantic pygmy pipehorse *Amphelikturus dendriticus* (Syngnathini; Hamilton et al. 2017; Stiller et al. 2022), indicating that this suite of characters has arisen multiple times within Syngnathidae.

Ventral pterygiophore evolution

The phylogenetic placement of *Australyichthys* within Haliichthyini invites comparison with *Acentronura*, *Idiotropiscis*, and *Cylix*, which together form the sister clade to *Hippocampus* (Hamilton et al. 2017; Stiller et al. 2022). CT examination of *A. gracilissima* (CAS 81986, male) reveals that this species shares several external characters with *Australyichthys*, including a head angled ventrally from the principal body axis, a prehensile tail, absence of a caudal fin, and development of a fully enclosed male brood pouch (Fig. S1; Dawson 1985; Short and Trnski 2021).

In male *A. gracilissima*, the brood pouch is positioned along the ventral midline of the tail and extends beneath the anteriormost 14 tail rings. CT reveals that enclosure is achieved by paired, bilaterally arranged brood pouch plates (BPP) situated on the first tail ring and projecting ventrolaterally from the anterior ventral plate ridges of successive tail rings, with elements diminishing progressively in size posteriorly (Fig. S1B; Short and Trnski 2021). Bilateral anal pouch plates (APP) are modified ventral plates associated with the pouch origin on the posteriormost trunk ring (Fig. S1B, C). Each APP is broad and paddle-shaped along its ventrocaudal margin and curves posterolaterally relative to the remaining brood pouch plates (Fig. S1C). Centered between, and structurally continuous with, the paired APPs is a pelvic-shaped median bone that curves ventroanteriorly. Two pterygiophores are positioned between this pelvic-shaped element (Fig. S1D), remaining integrated into the serial ventral plate complex.

The pterygiophores associated with the ventral pouch complex in *A. gracilissima* closely resemble the enlarged, composite anal pterygiophore described in *Australyichthys* and *Hippocampus*, in which the proximal radials are more or less rigidly bound together into a mechanically prominent element. The two pterygiophores in *A. gracilissima* are stacked vertically, as in *Hippocampus*, and possess bulbous, arrow-shaped termini. Comparative developmental and anatomical studies of *Hippocampus* indicate that skeletal muscle bundles associated with the anal fin assembly and its pterygiophores contribute directly to deformation of the pouch opening during parturition. Dudley et al. (2022) demonstrated that in *H. abdominalis*, the brood pouch epithelium contains only scattered small smooth muscle bundles, and in-vitro application of isotocin (a teleost nonapeptide hormone) does not produce measurable pouch contractions. Instead, CT and histological analysis revealed large skeletal muscle bundles attached to the anal fin bones at the male brood pouch opening, with two muscle pairs (depressors and inclinators) associated with each pterygiophore (Dudley

et al. 2022; Schneider et al. 2023). Parturition in *Hippocampus* is likely facilitated by contraction of these skeletal muscles, which, in combination with body movements, serves to gape open the pouch and expel neonates (Dudley et al. 2022). These studies support interpretation of the anal pterygiophore complex in *Hippocampus* as a mechanically integrated lever system acting in concert with associated skeletal musculature.

Similarly enlarged and integrated pterygiophores within the ventral pouch complex of *Acentronura* and *Australyichthys* indicate a shared structural framework for brood pouch mechanics within these lineages. In *Australyichthys*, a single median pterygiophore appears to represent fusion of multiple elements, whereas *Acentronura* retains two discrete pterygiophores stacked vertically; both configurations contrast with the three proximally discrete pterygiophores with fused termini retained in *Hippocampus*. This parallel reduction from three pterygiophores to one or two is observed in two genera within Haliichthyini (*Australyichthys*, *Acentronura*). This distribution raises the question of whether pterygiophore consolidation represents a synapomorphy of Haliichthyini, or whether it has arisen independently in *Acentronura* and *Australyichthys* in association with enclosed male brooding. The comparative data presented below begin to address this question, although two of three species of Pacific pygmy pipehorses (*Idiotropiscis* and *Cylix*) remain unexamined.

CT examination of *Haliichthys taeniophorus*, also recovered within Haliichthyini (Fig. 12), reveals three thick pterygiophores positioned internally within the anal ring at its posterior margin (Fig. S2). The pterygiophores are separated from each other but positioned between bones that form the posterior of the anal ring (Fig. S2B). The three pterygiophores are not fused as are the three in *Hippocampus*; they are unequal in size, with the largest element appearing to represent fusion of two proximal radials (Fig. S2C). The terminal ends of the pterygiophores in *H. taeniophorus* differ markedly from those observed in *Australyichthys*, *Hippocampus*, and *Acentronura*; rather than exhibiting bulbous termini, they are clavate with transverse ridges (Fig. S2C). Discrete, unfused pterygiophores in *H. taeniophorus*, which possesses a semi-exposed brood pouch and only a semi-prehensile tail at its distal tip, constitute a distinct departure from the fused pterygiophore morphology in genera with fully enclosed brood pouches and prehensile tails (*Hippocampus*, *Australyichthys*, *Acentronura*).

CT examination of *Halicampus grayi* (LSUMZ 18017), a pipefish also recovered within Haliichthyini, reveals three pterygiophores visible through the anal pore (Fig. S3). The pterygiophore termini taper to blunt tips rather than exhibiting the bulbous or clavate ends observed in other genera (Fig. S3B, C). Unlike in *Haliichthys taeniophorus*, the pterygiophores are positioned internally within the anal ring rather than embedded between its constituent bones. Three hook-like spines of varying length are also present (Fig. S3B, C). Despite possessing pterygiophores, the overall configuration differs markedly from *Haliichthys*. To assess pterygiophore morphology in pipefish lineages from phylogenetically distant tribes, we examined the trunk brooder *Syngnathus typhle* (UW 8205) from Syngnathini and *Choeroichthys brachysoma* (SLU 900) from Microphini; both possess two anal fin pterygiophores of varying shape, situated just posterior to the bones forming the anal ring (Figs. S4 and S5). Pterygiophore number and shape thus vary widely among pipefish genera, in configurations that appear genus-specific, suggesting that pterygiophore structure may be informative for generic delimitation within Syngnathidae.

Pterygiophore morphology in *Australyichthys*, *Acentronura*, and *Hippocampus* is strikingly similar: all three genera share enlarged pterygiophores with bulbous termini, combined with a prehensile tail, fully enclosed brood pouch, and ventrally angled head. By contrast, the non-prehensile *Halicampus grayi* possesses pterygiophores with blunt termini that differ markedly from this bulbous form.

Haliichthys taeniophorus, which possesses a semi-exposed brood pouch and only a loosely semi-prehensile tail at its distal tip, exhibits three unfused pterygiophores with a configuration that appears intermediate between pipefish and seahorse-like morphologies. If pterygiophore elaboration is linked to prehensility rather than pouch mechanics, taxa with enclosed pouches, but non-prehensile tails, would be predicted to lack enlarged pterygiophores. We hypothesize that pterygiophore enlargement could represent a derived structural modification associated with tail prehensility and mechanical stabilization of the trunk–tail junction during grasping. Selection acting on prehensile lineages may have favored skeletal reinforcement at the posterior trunk to redistribute torsional and compressive loads away from the brood pouch during anchoring, a selective pressure absent in non-prehensile pipefishes. The recurrence of similar pterygiophore morphology in phylogenetically independent lineages, *Hippocampus* in Hippocampini, and *Acentronura* and *Australyichthys* in Haliichthyini, suggests functional convergence and indicates that pterygiophore modification may be a predictable biomechanical response to the combined evolution of prehensile tails and enclosed brooding.

A potential biomechanical explanation concerns the constraints imposed by prehensile tail morphology on parturition. In pipefishes with caudal fins, body undulation may generate sufficient force to expel eggs or neonates from open or semi-enclosed pouches. Taxa with prehensile tails lack caudal fins and exhibit reduced axial flexibility, potentially limiting the effectiveness of undulation during parturition. The elaboration of anal pterygiophore-associated musculature in *Hippocampus*, *Acentronura*, and *Australyichthys* may represent a compensatory mechanism, providing skeletal leverage for pouch deformation in the absence of caudal propulsion. Under this hypothesis, pterygiophore consolidation and muscle elaboration are functionally linked to both pouch enclosure and tail prehensility, explaining their repeated co-occurrence. We stress that this scenario is a hypothesis derived entirely from comparative anatomy; no functional, kinematic, or biomechanical data were collected here, and it remains to be tested directly, including through the prediction set out below.

Apterygocampus epinnulatus Weber, 1913, the only pipefish known to possess a fully enclosed brood pouch yet lacking a prehensile tail (Dawson 1985), represents a critical test of this hypothesis. Unlike *Hippocampus*, *Acentronura*, and *Australyichthys*, this species retains the elongate pipefish body plan and non-prehensile tail, thereby decoupling pouch enclosure from tail prehensility. If pterygiophore elaboration is linked to prehensility rather than pouch enclosure alone, this species would likely lack the enlarged pterygiophores observed in prehensile taxa. Future anatomical examination of *A. epinnulatus* would clarify the evolutionary and functional integration of these characters across Syngnathidae.

Despite these similarities in pterygiophore structure, ventral trunk organization differs fundamentally between *Acentronura* and *Australyichthys*. In *Acentronura*, ventral plates are retained and contribute to brood pouch enclosure through development of anal pouch plates (APP) and brood pouch plates (BPP). In *Australyichthys*, ventral plates are entirely absent; the ventral trunk is instead supported by the derived AVE–PVE–MAP complex, which does not contribute to a continuous ventral ridge or enclosed pouch structure. The external similarity between these genera, including the seahorse-like body plan, prehensile tail, and enclosed brood pouch, therefore reflects convergent evolution of reproductive and locomotor adaptations rather than shared ancestry or homologous ventral trunk architecture.

Distinction from Hippocampus

The single most decisive contrast with *Hippocampus*, detailed in the *Diagnosis* and *Remarks* above, concerns the ventral trunk: *Hippocampus* encloses the body cavity in a rigid cylin-

der of inferior and ventral plates fused along the midline, whereas in *Australyichthys* ventral plates are absent, the inferior plates never meet at the midline, and ventral support is provided instead by the derived AVE–PVE–MAP complex—a configuration unknown elsewhere in Syngnathidae and the principal synapomorphy of the genus.

The derived ventral trunk skeleton of *Australyichthys* is closely integrated with reproductive anatomy. In males, embryos are positioned ventral to the posterior ventral elements (PVE) and immediately adjacent to the median anal pterygiophore (MAP), rather than being enclosed within a ventral brood chamber formed by fused ventral plates as in *Hippocampus*. The AVE–PVE–MAP complex forms a ventral scaffold that partially surrounds and supports developing embryos. This configuration differs fundamentally from the fully enclosed Type V brood pouch of *Hippocampus*, in which bilateral pouch walls meet and fuse along the ventral midline to form a sealed incubation chamber.

Species-level comparative variation

All species share the ventral trunk framework diagnostic of the genus but differ consistently in AVE segmentation, PVE fusion, ANP position, trunk-ridge development, and dermal-lobe

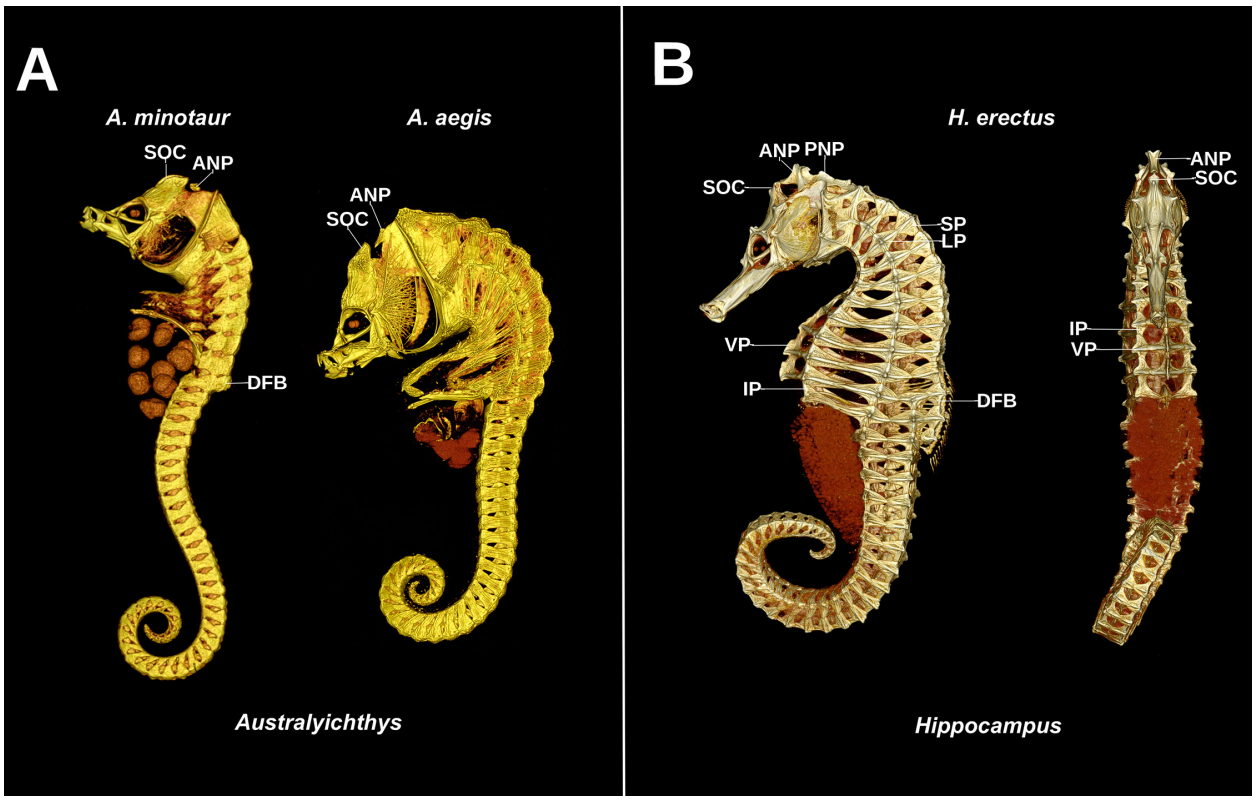

Figure 13. Comparative micro-CT images of *Australyichthys minotaur* (CSIRO H4464-01, male) and *A. aegis* (SAMA F14993, male) with *Hippocampus erectus* (UF 138664, male). Lateral and anterior views illustrate fundamental differences in trunk ossification, dorsal fin base (DFB) structure, embryo size and position (highlighted in red), and overall body configuration between *Australyichthys* and *Hippocampus*. In *Hippocampus*, the ventral midline is formed by continuous inferior and ventral plates, and the anal fin pterygiophore complex consists of three discrete radials. In *Australyichthys*, inferior plates remain unfused, ventral plates are absent, and the median anal pterygiophore (MAP) is interpreted as a consolidated homolog of the three-radial complex. Abbreviations: SOC = supraoccipital; ANP = anterior nuchal plate; PNP = posterior nuchal plate; SP = superior plate; LP = lateral plate; IP = inferior plate; VP = ventral plate; DFB = dorsal fin base; MAP = median anal pterygiophore; AVE = anterior ventral elements; PVE = posterior ventral elements.

morphology. In all three, ventral plates are absent and inferior trunk plates do not meet at the ventral midline; the ventral trunk is instead supported entirely by the AVE–PVE–MAP complex, conserved in organization but variable in configuration and articulation among species.

Despite this common structure, the AVE differ in number, segmentation, and longitudinal extent among species. In *A. paradoxus*, the AVE comprise multiple discrete ossifications extending along the ventrolateral margins of the anterior trunk, forming an elongated series associated with the anterior trunk rings. In *A. minotaur*, the AVE are expressed as a more compact, multisegmented series with reduced longitudinal extension relative to *A. paradoxus*. In *A. aegis*, the AVE are present as paired elements that are less extensively subdivided and more tightly associated with the anterior inferior plates. These differences in AVE configuration provide consistent characters for species-level discrimination within the genus.

Species-level variation is evident in the posterior ventral elements. In *A. paradoxus*, females exhibit two unfused, broad, spatulate PVE that flank a free-floating MAP. In *A. minotaur*, males bear paired elongate, rod-like PVE attached at trunk ring 8 with blunt distal termi-

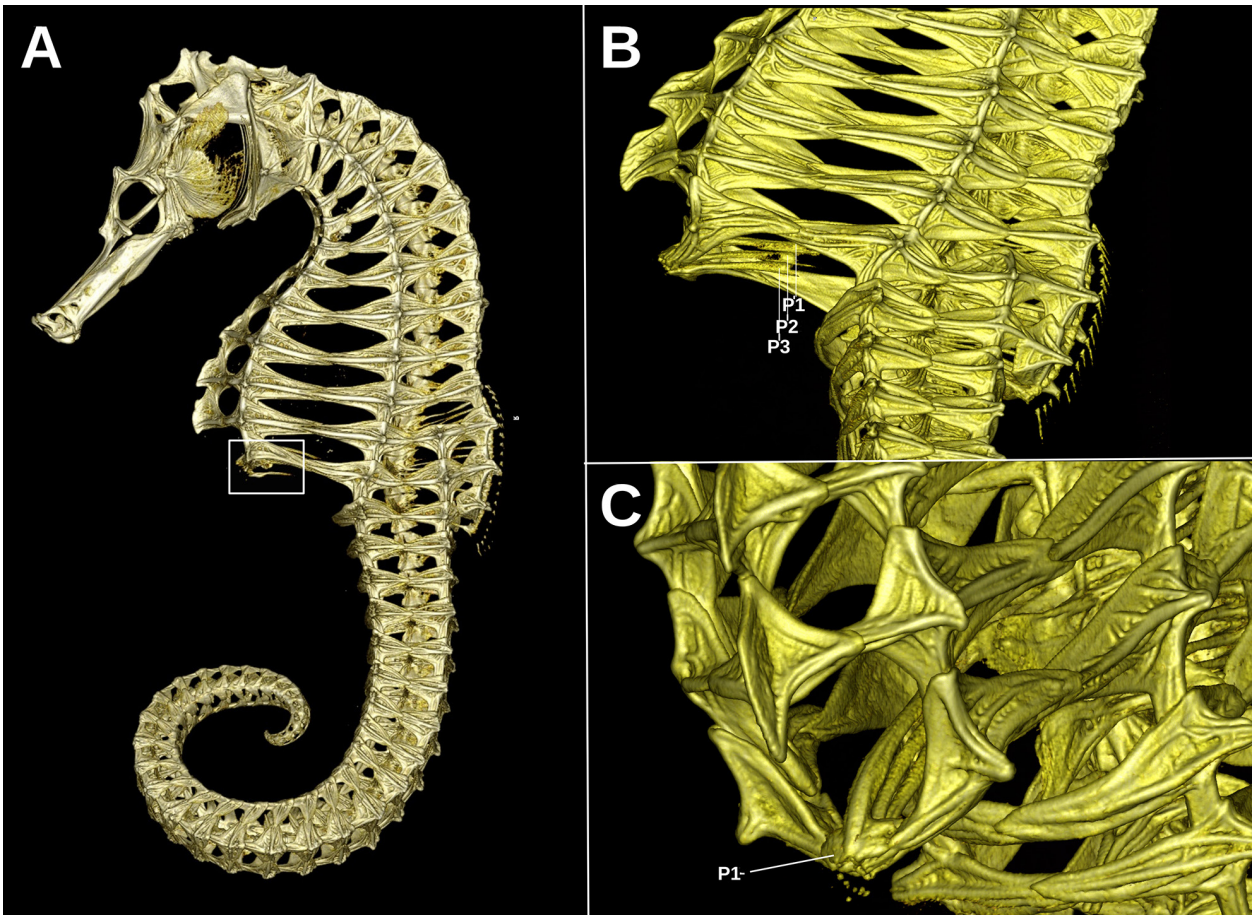

Figure 14. Micro-computed tomography (CT) scans showing anal-region osteology of *Hippocampus erectus* (UF 138664). (A) Ventral view of the posterior trunk showing the anal fin pterygiophore complex composed of three discrete radials arranged in a comb-like series at trunk ring 11. (B) Lateral view illustrating the positional relationship of the anal fin pterygiophores relative to the ventral trunk skeleton and inferior plates. Note the four distal radials of the anal fin marked by the white arrow. (C) Oblique ventrolateral view highlighting the stacked alignment of the pterygiophores with the dorsalmost proximal radial (P1) within the anal fin pterygiophore complex. Anterior to left. Abbreviations: P = pterygiophores.

ni, whereas females bear broad, spatulate PVE whose distal ends meet and fuse to the MAP. In *A. aegis*, males exhibit PVE that are fused proximally and separated distally, with the MAP positioned between the terminal ends. Across all species, however, the PVE occupy a homologous position relative to the posterior trunk and form the primary ventral supports underlying the brooding region. We suggest that the contrasting male and female PVE configurations in *A. minotaur* reflect variation in load-bearing and brood-support geometry rather than element number.

The MAP is present in all three species and occupies a central position within the ventral trunk complex, but its morphology and degree of integration with surrounding elements vary. In *A. paradoxus* and *A. minotaur*, the MAP is expressed as a single elongate ossification that extends posteriorly beneath the trunk and exhibits limited contact with adjacent ventral elements. In *A. aegis*, the MAP is more robust and exhibits closer spatial association with the PVE, resulting in a more integrated ventral scaffold.

The AVE, PVE, and MAP therefore operate at two levels: as a shared framework that diagnoses the genus, and, through differences in their number, segmentation, and spatial relationships, as characters that distinguish its species.

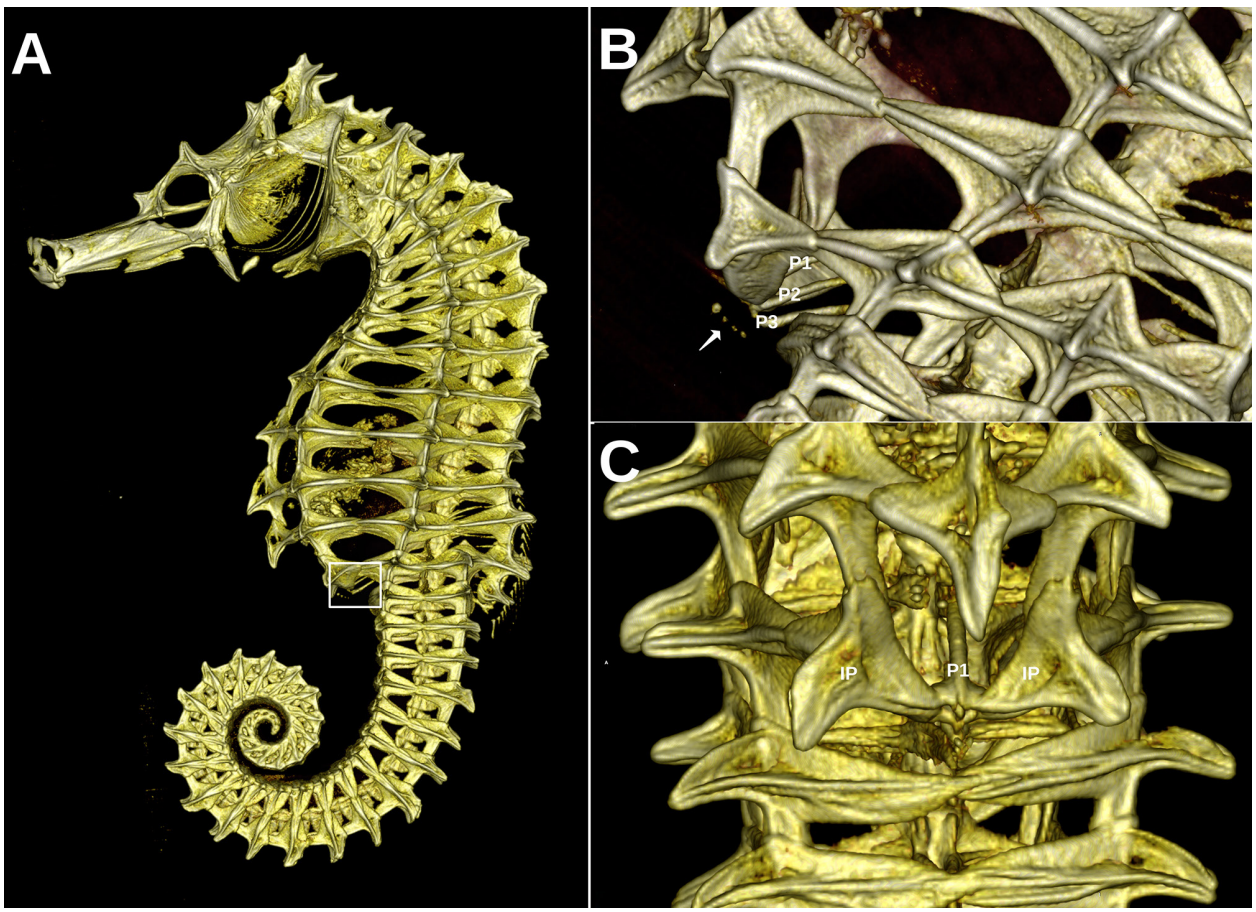

Figure 15. Micro-computed tomography (CT) three-dimensional reconstructions of the anal fin pterygiophore complex in *Hippocampus erectus* (UF 138664). (A) Ventral view showing the three-radial anal fin pterygiophore complex positioned along the ventral midline at trunk ring 11. (B) Lateral view illustrating the vertical stacking and spacing of the pterygiophores between the inferior plates of the posterior trunk. (C) Posteroventral oblique view emphasizing the stacked arrangement of the pterygiophores with the dorsalmost proximal radial (P1) within the ventral trunk. Anterior to left. Abbreviations: P = pterygiophores.

Geography

None of the three species has been recorded from inshore or shallow waters. *Australyichthys minotaur* occurs in southeastern Australia at known depths of 64–124 m, primarily off New South Wales and Victoria. *Australyichthys paradoxus* is known from 102 m depth in the Great Australian Bight, Western Australia, a region that includes rich bryozoan assemblages and wave-exposed calcareous substrates. *Australyichthys aegis*, the only species with genomic data, was collected from 50 m in Spencer Gulf, South Australia, near the lower mesophotic boundary as defined here. The genus spans multiple bioregions along southern Australia, as defined by the Integrated Marine and Coastal Regionalisation of Australia (IMCRA; Commonwealth of Australia 2006). This framework classifies Australia's marine environment into ecologically meaningful units based on the distribution of demersal fishes, marine invertebrates, seafloor geomorphology, and oceanographic data. *Australyichthys minotaur* occurs within the Twofold Shelf mesoscale bioregion of southeastern Australia, extending from Eden, New South Wales, into Bass Strait, Victoria. *Australyichthys aegis* is known from the Spencer Gulf Shelf Province, specifically near the Gambier and Neptune Islands at the entrance to Spencer Gulf, South Australia. *Australyichthys paradoxus* occurs within the Great Australian Bight Shelf Transition off Esperance, Western Australia. These bioregions are separated by wide continental shelf embayments such as the Great Australian Bight, with regional upwelling systems that include the Bonney Upwelling, as well as ecological transitions in substrate and benthic community structure that may act as dispersal barriers (Commonwealth of Australia 2006; James et al. 2001). These environmental discontinuities correspond to the geographic separation among species across more than 2,500 km of southern Australian coastline.

The distribution of *Australyichthys* is restricted to the mid-continental shelf, away from reef and estuarine zones typically occupied by shallow-water syngnathids. Among teleost fishes of southern Australia, *Australyichthys* appears, on present evidence, to be among the few lineages largely restricted to the temperate mesophotic zone, a pattern otherwise documented only for the handfish genus *Pezichthys* (Last and Gomon 2008), although this apparent restriction may partly reflect the limited sampling of mesophotic habitats. Species of *Pezichthys* are themselves typically highly range-restricted, a parallel that may bear on the narrow distributions and apparent rarity of *Australyichthys*.

STATUS

Evidence

We propose extending the lost species framework of Long and Rodríguez (2022), under which ten years without confirmed records in the wild is the suggested benchmark for declaring a taxon lost, from the species level to the generic level. Under this proposed extension, *Australyichthys* would qualify as a "lost genus," a designation we introduce here rather than one already formalized within that framework. All three species are known exclusively from historical museum specimens, and no individual of any species has been detected in the wild for nearly two decades, the most recent collection (*A. aegis*) dating to February 2006. The absence of verified *in situ* observations reflects the combined effects of apparent rarity, restriction to poorly surveyed mesophotic depths, and reliance on trawl bycatch as the sole collection method. Designation as lost in this context does not imply imminent extinction; it identifies a priority for targeted, non-extractive surveys of southern Australian mesophotic ecosystems to establish whether extant populations persist and to document the biology of this evolutionarily distinct lineage.

Search effort

All known specimens of *Australyichthys* were recovered incidentally as trawl or dredge by-

catch rather than through targeted survey effort. The genus is represented by only seven examined specimens collected over nearly eighty years across more than 2,500 km of southern Australian coastline, with the most recent collection in February 2006. No individual of any species has been observed *in situ*, and no targeted, non-extractive surveys of the temperate mesophotic habitats in which the genus occurs have been undertaken.

Threats

That every known specimen was taken incidentally as trawl bycatch, yet only seven have been recorded in nearly eighty years, suggests that *Australyichthys* occupies benthic microhabitats sampled only inefficiently by bottom trawls; this low catchability compounds the challenge of confirming persistence through fishery-dependent monitoring. Additional environmental pressures include ocean warming, deoxygenation, shifts in benthic community composition, and sedimentation from coastal activities, particularly in semi-enclosed systems such as Spencer Gulf where *A. aegis* was collected. Together, low catchability and these environmental pressures imply substantial vulnerability for a lineage confined to poorly surveyed mesophotic habitats.

The disjunct distribution of the three species across more than 2,500 km of the southern Australian coastline, from Eden, NSW, in the east to Esperance, WA, in the west, suggests that a formerly continuous mesophotic population may have fragmented during Pleistocene sea-level fluctuations that exposed the continental shelf. Whether early development includes a pelagic dispersal phase is unknown; data on egg size and larval duration, if obtainable from future material, could help evaluate the dispersal potential of *Australyichthys* across barriers such as the Great Australian Bight. If populations represent Pleistocene relicts, recolonization following local extinction is unlikely, amplifying the conservation significance of each isolated population. The collection method (trawl) and association with emergent invertebrate structure suggest *Australyichthys* is epibenthic rather than free-swimming or burrowing. Epibenthic species are disproportionately vulnerable to trawl impacts because they cannot escape into sediments or the water column, suggesting that the genus faces heightened risk from bottom-contact fishing relative to other syngnathids.

Rediscovery strategy

Efforts to locate extant populations should prioritize mesophotic depths corresponding to the collection localities of the three species. The most plausible sites for *A. minotaur* lie off Eden and the southern New South Wales coast. *Australyichthys paradoxus* is known only from the western Great Australian Bight, while *A. aegis* is associated with the Gambier and Neptune Islands at the entrance to Spencer Gulf. These regions share benthic communities dominated by bryozoans, sponges, and soft corals, matching the habitat descriptions provided by James et al. (2001) for the holotype of *A. paradoxus*. Visual searches will require mesophotic diving because the diminutive size and cryptic profile of these fishes reduce detectability using remotely operated vehicles. Pygmy seahorses have, however, been observed in situ using a remotely operated vehicle (ROV) (D. Harasti pers. comm. 2025). Remote systems nonetheless provide high-resolution mapping of habitat structure and facilitate non-destructive documentation of associated fauna. Environmental DNA may complement these approaches, although detection is likely constrained by low population density; the genomic data generated for *A. aegis* in this study provide a foundation for eDNA primer development, and sequencing of additional species from existing museum material would further enhance molecular detection capability. Seasonal timing may influence detection, as gravid males collected during austral spring and summer suggest increased activity or visibility during this period. Marine protected areas such as the Great Australian Bight Ma-

rine Park and Gambier Islands Group Marine Park offer optimal sites for systematic surveys free from active trawling.

CONCLUSION

The description of *Australyichthys* gen. nov. reveals a previously unrecognized lineage of syngnathid fishes restricted to temperate mesophotic ecosystems of southern Australia. Phylogenomic analysis places the genus within Haliichthyini, demonstrating that its seahorse-like external morphology, including the ventrally angled head, prehensile tail, and fully enclosed brood pouch, evolved independently from *Hippocampus*. CT-based osteological analysis reveals a suite of synapomorphic characters, including the AVE–PVE–MAP ventral trunk support complex, that distinguish *Australyichthys* from all other syngnathid genera. Comparison across Haliichthyini and Hippocampini indicates that the co-occurrence of enclosed brooding, tail prehensility, and elaborated anal pterygiophore architecture has evolved repeatedly within Syngnathidae and may represent a functionally integrated character complex associated with the biomechanics of parturition. The genus expands the documented diversity of Australia's mesophotic ecosystems and identifies a clear target for expanded survey effort and comparative anatomical study across Syngnathidae.

The designation of *Australyichthys* as a lost genus extends the lost species framework to marine mesophotic fishes, a group for which this framework has rarely been applied. Unlike terrestrial lost species, which may persist in remote but potentially accessible refugia, mesophotic marine taxa occupy habitats that impose fundamental barriers to detection: depth, specialized survey requirements, and the logistical constraints of technical diving. These constraints compound uncertainty about population status and make dedicated mesophotic survey infrastructure a prerequisite for any reliable assessment.

ORCID

G.S. 0000-0002-4691-1913
R.F. 0009-0007-4872-1631
M.G. 0000-0001-9896-1173
S.B. 0000-0002-7309-2095
C.M.S. 0000-0003-1615-7590
H.H. 0000-0002-4368-0101
A.D. 0009-0007-0285-3970
D.H. 0000-0002-2851-9838
K.P. 0000-0003-1866-8650
A.H. 0000-0002-1335-2342

Data accessibility

Newly generated whole-genome shotgun sequence data and ultraconserved element (UCE) sequences for *Australyichthys aegis* sp. nov. (SAMA F14993; tissue bank registration ABTC137691) have been deposited in GenBank (National Center for Biotechnology Information), with accession numbers as follows: BioProject PRJNA1494570 and BioSample SAMN61611572. Existing UCE alignments for comparative syngnathid taxa were obtained from EMBL-EBI BioProject PRJNA734786 (Stiller et al. 2022). All physical type and voucher specimens are permanently deposited in the ichthyological collections of the South Australian Museum (SAMA), Australian Museum (AMS), Museums Victoria (NMV), CSIRO Australian National Fish Collection, and California Academy of Sciences (CAS), as detailed in the Materials Examined sections. Existing UCE alignments for comparative syngnathid taxa were obtained from EMBL-EBI BioProject PRJNA734786 (Stiller et al. 2022). Micro-computed tomography (CT) scan data for *Australyichthys aegis* (SAMA F14993), *A. minotaur* (CSIRO H4464-01), *A. paradoxus* (SAMA F10490), and comparative material of *Hippocampus erectus* (UF 138664), generated at the Karel F. Liem BioImaging Center, Friday Harbor Laboratories, University of Washington, are available from the corresponding author upon reasonable request. All physical type and voucher specimens are permanently deposited in the ichthyological collections of the South Australian Museum (SAMA), Australian Museum (AMS), Museums Victoria (NMV), CSIRO Australian National Fish Collection, and California Academy of Sciences (CAS), as detailed in the Materials examined.

Author contributions

G. Short, project conception, CT imaging, writing of the original draft, and manuscript editing; R. Foster, project conception, curatorial assistance, manuscript editing, and access to NMV holotype

of *A. aegis*; M. Gomon, curatorial assistance, manuscript editing, and access to SAMA holotype of *A. minotaur*; S. Bassham and C. M. Small, phylogenomic and bioinformatic analysis, and manuscript editing; H. Hamilton, discussion of project details and mesophotic ecosystems, and manuscript editing; A. DuToit, analysis of pterygiophore segmentation in syngnathids for comparison with the new genus, and manuscript editing; D. Harasti, discussion of project details and mesophotic ecosystems in NSW, and manuscript editing; C. Biggs, discussion of project details, mesophotic ecosystems, and the history of *A. minotaur* in southern NSW (Eden), and manuscript editing; K. Parkinson, curatorial assistance, CT scanning and imaging of AMS *A. minotaur* paratypes, manuscript editing, and access to AMS specimens; A. Hay, curatorial assistance, manuscript editing, access to AMS specimens, and proposal of the common name "sea Muppet".

Ethical standards and competing interests

This study was based on existing museum specimens, and no new field collection was undertaken by the authors. Access to type and voucher specimens was granted by the holding institutions (South Australian Museum, Australian Museum, Museums Victoria, CSIRO Australian National Fish Collection, and California Academy of Sciences). Genomic sampling was conducted on archived tissue under the relevant institutional protocols. No permits or institutional animal-ethics approvals were required for this work, and the authors declare no competing interests.

Acknowledgements

We thank the following museum curators and collection managers for providing access to specimens essential to this study: A. Hay, K. Parkinson, S. Reader (Australian Museum); D. Catania and M. Hoang (California Academy of Sciences); A. Graham (CSIRO); and D. Bray (Museum Victoria), and K. Maslenikov (School of Aquatic and Fishery Sciences and Burke Museum of Natural History and Culture, University of Washington). For technical and analytical support, we are grateful to A. King (Australian Centre for Wildlife Genomics, AMS) for genomic DNA extraction from *A. aegis,* J. Bishop (University of Oregon's Genomics and Cell Characterization Core Facility, UO) for genomic library preparation from genomic DNA extracted from *A. aegis,* and to C. Goatley (UOS) for CT scan data of non-type material of *Australyichthys*. We also thank B. Cresko (University of Oregon) for facilitating the inclusion of *A. aegis* in sequencing efforts, enabling generation of genomic data for this study. We are also grateful to J. Stiller, whose phylogenomic study of Syngnathidae provided the ultraconserved element (UCE) dataset that aided in resolving the phylogenetic placement of the new genus. H. O'Neill (CSIRO) provided excellent photographs of non-type material of *A. minotaur*, significantly enhancing the documentation. Special thanks to D. Muirhead for convivial discussion on syngnathid diversity in South Australia. We appreciate the thorough reviews and constructive feedback from our JLS editors and anonymous reviewers, which improved this manuscript. This research was primarily supported by GS's Australian Museum Foundation/ AMI Visiting Collections Fellowship at the Australian Museum in 2022, hosted by A. Hay.

Supplementary material

Additional material associated with this article is available online and includes images and morphological diagrams of focal taxa (Figs. S1–S5).

Literature cited

Adams LA, Karenyi N, Parker D, Sink K. 2023. Patterns and potential drivers of mesophotic communities of the warm-temperate Amathole shelf of South Africa. *Estuarine, Coastal and Shelf Science* 295: 108562. doi:10.1016/j.ecss.2023.108562

Ahmadia GN, Sheard LJ, Pezold FL, Smith DJ. 2012. Cryptobenthic fish assemblages across the coral reef–seagrass continuum in SE Sulawesi, Indonesia. *Aquatic Biology* 16(2): 125–135. doi:10.3354/ab00440

Baker JL. 2006. Syngnathid fish (seahorses, seadragons, pipehorses and pipefishes). Pages 227–280 in Benthos Survey of 12 Sites in the South Australian Marine Parks Pilot Project, Volume 1 – Results for Individual Sites. Prepared for the Coast and Marine Conservation Branch, Department for Environment and Heritage, Adelaide.

Bastiaansen A, Barrett N, Perkins N, Monk J, Strain EM. 2024. Taking a deeper look at the biodiversity on temperate mesophotic reefs to inform adaptive management of impacts in Storm Bay, Tasmania. *Ecological Indicators* 166: 112345. doi:10.1016/j.ecolind.2024.112345

Bell JJ, Micaroni V, Harris B, Strano F, Broadribb M, Rogers A. 2024. Global status, impacts, and management of rocky temperate mesophotic ecosystems. *Conservation Biology* 38(1): e13945. doi:10.1111/cobi.13945

Beran H. 2024. Diving deep to escape the heat: the importance of mesophotic reefs as thermal refuges for New Zealand coastal fishes. PhD thesis, Victoria University of Wellington.

Baine MSP, Barrows APW, Ganiga G, Martin-Smith KM. 2008. Residence and movement of pygmy seahorses, *Hippocampus bargibanti*, on sea fans (*Muricella* spp.). *Coral Reefs 27*(2): 421. doi:10.1007/s00338-007-0352-5

Bongaerts P, Smith TB. 2019. Beyond the "Deep Reef Refuge" hypothesis: a conceptual framework to characterize persistence at depth. Pages 881–895 in Loya Y, Puglise KA, Bridge TCL, eds. Mesophotic Coral Ecosystems. Coral Reefs of the World, vol. 12. Springer, Cham. doi:10.1007/978-3-319-92735-0_45

Brandl SJ, Goatley CHR, Bellwood DR, Tornabene L. 2018. The hidden half: ecology and evolution of cryptobenthic fishes on coral reefs. *Biological Reviews* 93: 1846–1873. doi:10.1111/brv.12423

Bridge TCL, Hughes TP, Guinotte JM, Bongaerts P. 2013. Call to protect all coral reefs. *Nature Climate Change* 3: 528–530. doi:10.1038/nclimate1879

Browne RK, Baker JL, Connolly RM. 2008. Syngnathids: seadragons, seahorses and pipefish. Pages 162–176 in Shepherd SA, Bryars S, Kirkegaard I, Harbison P, Jennings JT, eds. Natural History of Gulf St Vincent. Royal Society of South Australia, Adelaide.

Commonwealth of Australia. 2006. A Guide to the Integrated Marine and Coastal Regionalisation of Australia Version 4.0. Department of the Environment and Heritage, Canberra.

Currey-Randall LM, Galaiduk R, Stowar M, Vaughan BI, Miller KJ. 2021. Mesophotic fish communities of the ancient coastline in Western Australia. *PLOS ONE 16*(4): e0250427. doi:10.1371/journal.pone.0250427

Dawson CE. 1985. Indo-Pacific pipefishes (Red Sea to the Americas). Gulf Coast Research Laboratory, Ocean Springs, Mississippi.

Dawson CE, Allen GR. 1978. Synopsis of the 'finless' pipefish genera (*Penetopteryx*, *Apterygocampus* and *Enchelyocampus*, gen. nov.). *Records of the Western Australian Museum* 6(4): 391–411.

Department for Environment and Heritage. 2008. Towards a system of ecologically representative marine protected areas in South Australian marine bioregions. Government of South Australia.

Department for Environment and Heritage. 2009. Gambier Islands Group Marine Park: Draft management plan summary. Government of South Australia, Adelaide.

Department of Environment, Water and Natural Resources. 2012a. Gambier Islands Group Marine Park Management Plan 2012. Government of South Australia, Adelaide.

Department of Environment, Water and Natural Resources. 2012b. South Australia's marine parks: a shared vision. Government of South Australia, Adelaide.

Dudley JS, Paul JW, Teh V, Mackenzie TE, Butler TA, Tolosa JM, Smith R, Foley M, Dowland S, Thompson MB, Whittington CM. 2022. Seahorse brood pouch morphology and control of male parturition in *Hippocampus abdominalis*. *Placenta* 127: 88-94. doi:10.1016/j.placenta.2022.07.015

Foster R, Gomon MF. 2010. A new seahorse (*Hippocampus paradoxus*) from south-western Australia. *Zootaxa* 2613: 61–68. doi:10.11646/zootaxa.2613.1.6

Gomon MF. 1997. *Hippocampus minotaur*, a new seahorse from south-eastern Australia. *Memoirs of the Museum of Victoria* 56: 245–253. doi:10.24199/j.mmv.1997.56.10

Gomon MF, Bray DJ, Kuiter RH. 2008. Fishes of Australia's Southern Coast. New Holland, Chatswood.

Gragnolati M, Rolim FA, Pereira-Filho GH, Athayde ACS, Ciotti ÁM, Motta FS. 2024. Vertical structure of reef fish assemblages and light penetration reveal new boundaries of mesophotic ecosystems in the subtropical Southwestern Atlantic. *Marine Environmental Research* 198: 106527. doi:10.1016/j.marenvres.2024.106527

Hamilton H, Saarman N, Short G, Sellas AB, Moore B, Hoang T, Grace CL, Gomon M, Crow K, Simison WB. 2017. Molecular phylogeny and patterns of diversification in syngnathid fishes. *Molecular Phylogenetics and Evolution* 107: 388–403. doi:10.1016/j.ympev.2016.10.003

Harris B, Davy SK, Bell JJ. 2021. Benthic community composition of temperate mesophotic ecosystems in New Zealand. *Marine Ecology Progress Series* 671: 21–43. doi:10.3354/meps13758

Hoang DT, Chernomor O, von Haeseler A, Minh BQ, Vinh LS. 2018. UFBoot2: improving the ultrafast bootstrap approximation. *Molecular Biology and Evolution* 35: 518–522. doi:10.1093/molbev/msx281

Hoese DF, Bray DJ, Paxton JR, Allen GR. 2006. Fishes. Pages 1–2178 in Beesley PL, Wells A, eds. *Zoological Catalogue of Australia.* Volume 35. ABRS & CSIRO Publishing, Australia, parts 1–3.

Huang YH, Sun YF, Li H, Li HS, Pang H. 2024. PhyloAln: a convenient reference-based tool to align sequences and high-throughput reads for phylogeny and evolution in the omic era. *Molecular Biology and Evolution* 41(7): msae150. doi:10.1093/molbev/msae150

James NP, Bone Y, Collins LB, Kyser TK. 2001. Surficial sediments of the Great Australian Bight. *Journal of Sedimentary Research* 71: 549–567. doi:10.1306/102000710549

Kalyaanamoorthy S, Minh BQ, Wong TKF, von Haeseler A, Jermiin LS. 2017. ModelFinder: fast model selection for accurate phylogenetic estimates. *Nature Methods* 14: 587–589. doi:10.1038/nmeth.4285

Kikinis R, Pieper SD, Vosburgh KG. 2013. 3D Slicer: a platform for subject-specific image analysis, visualization, and clinical support. Pages 277–289 in Jolesz FA, ed. Intraoperative Imaging and Image-Guided Therapy. Springer, New York, NY. doi:10.1007/978-1-4614-7657-3_19

Kuiter RH. 2001. Seahorses, pipefishes and their relatives. TMC Publishing, Chorleywood.

Last PR, Gomon MF. 2008. Handfishes. Pages 518–521 in Gomon MF, Bray DJ, Kuiter RH, eds. Fishes of Australia's Southern Coast. Reed New Holland, Chatswood, Australia.

Last PR, White WT, Gledhill DC, Hobday AJ, Brown R, Edgar GJ, Pecl G. 2011. Long-term shifts in abundance and distribution of a temperate fish fauna. *Global Ecology and Biogeography* 20: 58–72.

Loiseau N, Villéger S, Le Bozec C, Gimenez M, Kawahara SL, Claverie T. 2023. Mesophotic reefs are not refugia for reef-fish diversity. *Coral Reefs* 42: 63–75. doi:10.1007/s00338-022-02311-1

Long B, Rodríguez JP. 2022. Lost but not forgotten: a new nomenclature to support a call to rediscover and conserve lost species. *Oryx* 56: 481–482. doi:10.1017/S0030605322000618

Lourie SA, Kuiter RH. 2008. Three new pygmy seahorse species from Indonesia. *Zootaxa* 1963: 54–68. doi:10.11646/zootaxa.1963.1.4

Lourie SA, Pollom RA, Foster SJ. 2016. A global revision of the seahorses *Hippocampus* Rafinesque, 1810 (Actinopterygii: Syngnathiformes): taxonomy and biogeography with recommendations for further research. *Zootaxa* 4146(1): 1–66. doi:10.11646/zootaxa.4146.1.1

Lourie SA, Randall JE. 2003. A new pygmy seahorse, *Hippocampus denise* (Teleostei: Syngnathidae), from the Indo-Pacific. *Zoological Studies* 42(2): 284–291.

Martin-Smith KM. 2003. Role of syngnathids in shallow coastal ecosystems of southeastern Australia. Pages 89–100 in Forrest RE, Scandol JP, Pitcher TJ, eds. Towards Ecosystem-based Fishery Management in New South Wales – Proceedings of the Experts and Data Workshop. Fisheries Centre Research Reports. Fisheries Centre, University of British Columbia, Vancouver, BC, Canada.

Minh BQ, Schmidt HA, Chernomor O, Schrempf D, Woodhams MD, von Haeseler A, Lanfear R. 2020. IQ–TREE 2: new models and efficient methods for phylogenetic inference in the genomic era. *Molecular Biology and Evolution* 37(5): 1530-1534. doi:10.1093/molbev/msaa015

Moore G, Ritchie J, Nester G, Kendrick A. 2024. Spatio-temporal distribution of syngnathid fishes in Cockburn Sound and Owen Anchorage, Western Australia. Western Australian Marine Science Institution, Perth.

Navarro Campoy A, Pérez-Matus A, Wieters EA, Alarcón-Ireland R, Garmendia V, Beldade R, Navarrete SA, Fernández M. 2023. The hidden diversity of temperate mesophotic ecosystems from central Chile (Southeastern Pacific Ocean) assessed through towed underwater videos. *Diversity* 15(3): 360. doi:10.3390/d15030360

Neira FJ, Miskiewicz AG, Trnski T. 1998. Larvae of Temperate Australian Fishes: Laboratory Guide for Larval Fish Identification. University of Western Australia Press, Nedlands, 474 pp.

Peter KL, Harris JH, Gehrke PC. 2011. Assessing the fish assemblages in seagrass meadows in the lower Murray River, South Australia. Report prepared for the South Australian Murray–Darling Basin Natural Resources Management Board, Adelaide, South Australia.

Rambaut A. 2018. FigTree. Version 1.4.4. http://tree.bio.ed.ac.uk/software/figtree/ (accessed 1 Mar 2026).

Rolfe S, Pieper S, Porto A, Diamond K, Winchester J, Shan S, Kirveslahti H, Boyer D, Summers A, Maga AM. 2021. SlicerMorph: an open and extensible platform to retrieve, visualize and analyze 3D morphology. *Methods in Ecology and Evolution* 12(10): 1816–1825. doi:10.1111/2041-210X.13669

Sabaj MH. 2020. Codes for natural history collections. *Copeia* 108: 593–669. doi:10.1643/ASIHCODONS2020

Sayyari E, Mirarab S. 2016. Fast coalescent-based computation of local branch support from quartet frequencies. *Molecular Biology and Evolution* 33: 1654–1668. doi:10.1093/molbev/msw079

Schneider RF, Woltering JM, Adriaens D, Roth O. 2023. A comparative analysis of the ontogeny of syngnathids (pipefishes and seahorses) reveals how heterochrony contributed to their diversification. *Developmental Dynamics* 252(5): 553–588. doi:10.1002/dvdy.551

Short G, Smith R, Motomura H, Harasti D, Hamilton H. 2018. *Hippocampus japapigu*, a new species of pygmy seahorse from Japan, with a redescription of *H. pontohi* (Teleostei, Syngnathidae). *ZooKeys* 779: 27–49. doi:10.3897/zookeys.779.24799

Short G, Claassens L, Smith R, De Brauwer M, Hamilton H, Stat M, Harasti D. 2020. *Hippocampus nalu*, a new species of pygmy seahorse from South Africa, and the first record of a pygmy seahorse from the Indian Ocean (Teleostei, Syngnathidae). *ZooKeys* 934: 141–156. doi:10.3897/zookeys.934.50924

Short GA, Trnski T. 2021. A new genus and species of pygmy pipehorse from Taitokerau Northland, Aotearoa New Zealand, with a redescription of *Acentronura* Kaup, 1853 and *Idiotropiscis* Whitley, 1947 (Teleostei, Syngnathidae). *Ichthyology & Herpetology 109*(3): 806–835. doi:10.1643/i2020136

Smith RE, Grutter AS, Tibbetts IR. 2012. Extreme habitat specialisation and population structure of two gorgonian-associated pygmy seahorses. *Marine Ecology Progress Series 444*: 195–206. doi:10.3354/meps09471

Stiller J, Short G, Hamilton H, Saarman N, Longo S, Wainwright P, Rouse GW, Simison WB. 2022. Phylogenomic analysis of Syngnathidae reveals novel relationships, origins of endemic diversity and variable diversification rates. *BMC Biology* 20(1): 75. doi:10.1186/s12915-022-01271-w

Turner JA, Andradi-Brown DA, Gori A, Bongaerts P, Burdett HL, Ferrier-Pagès C, Voolstra CR, Weinstein DK, Bridge TC, Costantini F, Gress E. 2019. Key questions for research and conservation of mesophotic coral ecosystems and temperate mesophotic ecosystems. Pages 989–1003 in Loya Y, Puglise KA, Bridge TCL, eds. Mesophotic Coral Ecosystems. Springer, Cham. doi:10.1007/978-3-319-92735-0_49

Williams J, Jordan A, Harasti D, Davies P, Ingleton T. 2019. Taking a deeper look: Quantifying the differences in fish assemblages between shallow and mesophotic temperate rocky reefs. *PlOS ONE 14*(3): e0206778. doi.org/10.1371/journal.pone.0206778

Wilson AB, Vincent ACJ, Ahnesjö I, Meyer A. 2001. Male pregnancy in seahorses and pipefishes (Family Syngnathidae): rapid diversification of paternal brood pouch morphology inferred from a molecular phylogeny. *Journal of Heredity* 92(2): 159–166. doi:10.1093/jhered/92.2.159

Wong RH, Monk J, Perkins NR, Barrett NS. 2023. Anthropogenic stressors on mesophotic reef communities. *Frontiers in Marine Science* 10: 1276072. doi:10.3389/fmars.2023.1276072

Yearsley GK, Last PR, Hoese DF. 2006. Standard names of Australian fishes. CSIRO Marine and Atmospheric Research Paper No. 9. Hobart: CSIRO Marine and Atmospheric Research. 64 pp.

Zhang C, Mirarab S. 2022. Weighting by gene tree uncertainty improves accuracy of quartet-based species trees. *Molecular Biology and Evolution* 39: msac215. doi:10.1093/molbev/msac215